Molecular Cell, Vol. 9, 1017–1029, May, 2002, Copyright ©2002 by Cell Press

E2F1 and c-Myc Potentiate Apoptosis through Inhibition of NF-κB Activity that Facilitates MnSOD-Mediated ROS Elimination

Hirokazu Tanaka,[1,2,5] Itaru Matsumura,[1,4,5] Sachiko Ezoe,[1] Yusuke Satoh,[1] Toshiyuki Sakamaki,[3] Chris Albanese,[3] Takashi Machii,[1] Richard G. Pestell,[3] and Yuzuru Kanakura[1]

[1]Department of Hematology/Oncology
Osaka University Graduate School of Medicine
2-2 Yamada-oka, Suita
Osaka 565-0871

[2]Foundation for Biomedical Research and Innovation
6-1 Minatojimanakamachi, Chuo-ku
Kobe, Hyogo 650-8543
Japan

[3]The Albert Einstein Cancer Center
Department of Developmental and Molecular Biology and Department of Medicine
Albert Einstein College of Medicine
Bronx, New York 10461

Summary

Overexpression of c-Myc or E2F1 sensitizes host cells to various types of apoptosis. Here, we found that overexpressed c-Myc or E2F1 induces accumulation of reactive oxygen species (ROS) and thereby enhances serum-deprived apoptosis in NIH3T3 and Saos-2. During serum deprivation, MnSOD mRNA was induced by NF-κB in mock-transfected NIH3T3, while this induction was inhibited in NIH3T3 overexpressing c-Myc or E2F1. In these clones, E2F1 inhibited NF-κB activity by binding to its subunit p65 in competition with a heterodimeric partner p50. In addition to overexpressed E2F1, endogenous E2F1 released from Rb was also found to inhibit NF-κB activity in a cell cycle-dependent manner by using E2F1$^{+/+}$ and E2F1$^{-/-}$ murine embryonic fibroblasts. These results indicate that E2F1 promotes apoptosis by inhibiting NF-κB activity.

Introduction

Cell growth and differentiation are regulated in a cell cycle-dependent manner. Cell cycle machinery also controls cell survival and death. In general, cell cycle progression makes various types of cells susceptible to death. E2F1, a founding member of E2F family proteins (E2F1-6), is a direct executor of G1/S transition (Sherr and Roberts, 1999). E2F1 forms complexes with DP-1 family proteins and induces various genes required for G1/S transition. E2F1 activity is regulated by its interaction with Rb family proteins. At early-G1, dephosphorylated Rb binds to E2F1 and inhibits its activity. During mid-G1, Rb is sequentially phosphorylated by cyclin-dependent kinases and then releases E2F1, which initiates transcription of its target genes. In addition to the roles as a cell cycle regulator, E2F1 enhances various types of apoptosis in vitro and in vivo (Harbour and Dean, 2000). Although E2F1 has been shown to potentiate apoptosis through the induction of proapoptotic genes such as p73, ARF, caspase 3, and Apaf-1 (Bates et al., 1998; Zindy et al., 1998; Irwin et al., 2000; Lissy et al., 2000; Moroni et al., 2001; Muller et al., 2001), it was also reported that mutant E2F1 lacking transcriptional activity could enhance apoptosis as effectively as wild-type (wt) E2F1 (Hsieh et al. 1997; Phillips et al., 1997). Therefore, it is not well understood how E2F1 sensitizes host cells to apoptosis. Moreover, it is well known that c-Myc, another type of key regulator of G1/S transition, potentiates various apoptosis (Dang, 1999). c-Myc is overexpressed in malignant cells such as Burkitt lymphoma and multiple myeloma. In addition, c-Myc and/or E2F1 were supposed to be expressed at high levels in normal cells during developmental process in the adult body and in recovering tissues (e.g., various types of cells after injury and hematopoietic cells after chemotherapy). So, it is necessary to clarify the roles of c-Myc and E2F1 in the regulation of cell survival for the better understanding of biologic properties of these rapidly proliferating cells.

Reactive oxygen species (ROS), including superoxide anions, H_2O_2, organic peroxides, and hydroxyl radicals, are by-products of oxidative phosphorylation and constantly generated in all aerobic cells during normal metabolism (Adler et al., 1999; Rhee, 1999). Although ROS are required for the physiologic function of the cells, excessive ROS cause apoptosis through several mechanisms such as activation of JNK (c-Jun N-terminal kinase), disruption of mitochondrial membrane potential ($\Delta\Psi m$), and/or direct activation of caspase cascades (Cai et al., 1998). Under normal circumstances, ROS are eliminated by antioxidant enzymes. The scavenger enzyme, superoxide dismutase (SOD) (MnSOD or Cu/ZnSOD), converts superoxide anions to H_2O_2. H_2O_2 is subsequently detoxified by catalase or glutathione peroxidase (Adler et al., 1999; Rhee, 1999). This redox regulation is essential for protecting cells from apoptosis.

Apoptosis is also regulated by transcription factors named the Rel/NF-κB family that includes five members (c-Rel, p65 [RelA], RelB, p50, and p52) (Barkett and Gilmore, 1999). Although these members form homodimers or heterodimers in various combinations, a heterodimer p65/p50 is the most common form in mammalian cells and is specifically called NF-κB. NF-κB is retained in cytoplasm by its inhibitor IκB proteins as an inactive complex. Various stimuli such as proinflammatory cytokines and viruses activate the IκB kinase (IKK) complex and phosphorylate IκB. Upon phosphorylation, IκB is degraded by ubiquitin/proteasome pathways. The released NF-κB enters nucleus, binds to the target DNA, and initiates transcription. NF-κB is known to promote the expression of over 150 target genes that regulate immune response, stress response, or apoptosis. As for apoptosis, NF-κB plays a central role in its prevention through the induction of antiapoptotic genes such as Bcl-XL, c-IAP1, c-IAP2, and A1/Bfl1 (Barkett and Gilmore, 1999). In fact, p65$^{-/-}$ mice were embryonic lethal due to apoptosis of hepatocytes (Beg et al., 1995), and

[4]Correspondence: matumura@bldon.med.osaka-u.ac.jp
[5]These authors contributed equally to this work.

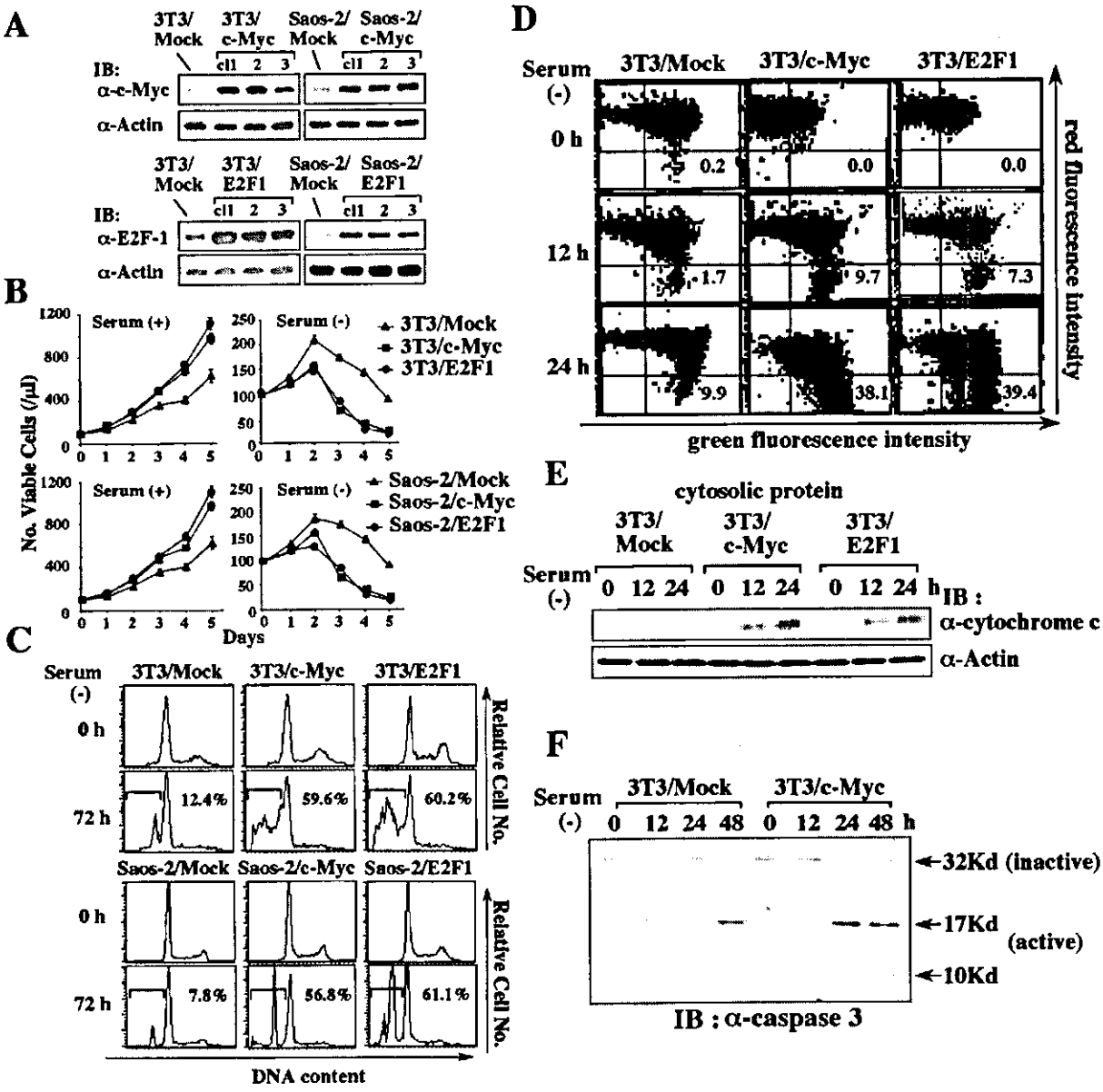

Figure 1. Effects of c-Myc and E2F1 on the Growth and Survival of NIH3T3 and Saos-2

(A) The expression levels of c-Myc and E2F1 were examined by immunoblot analysis. IB, immunoblot.

(B) Total number of viable cells were counted by trypan blue dye exclusion method. The results are shown as mean ± SD of triplicated cultures.

(C) DNA content of the cultured cells was examined by PI staining. The proportion of the sub-G1 fraction is indicated.

(D) $\Delta\Psi m$ was analyzed by flow cytometry. The cells with the decreased $\Delta\Psi m$ were detected in the lower right area. The proportion of the cells in this area is indicated.

(E and F) The release of cytochrome c into cytosol and activation of caspase 3 were evaluated by immunoblot analyses.

the cells from these mice were susceptible to apoptosis induced by various reagents (Barkett and Gilmore, 1999).

Here, we examined the relationship between cell cycle control and apoptosis in NIH3T3 and Saos-2 cells overexpressing c-Myc or E2F1 and found that their overexpression induced ROS accumulation and promoted serum-deprived apoptosis. Furthermore, E2F1 was found to suppress ROS-induced MnSOD expression by inhibiting NF-κB activity. These results indicate that E2F1 would potentiate apoptosis by inhibiting cell survival signals.

Results

c-Myc and E2F1 Sensitize NIH3T3 and Saos-2 to Serum-Deprived Apoptosis

We overexpressed c-Myc and E2F1 in NIH3T3 and Saos-2; each clone was designated 3T3/c-Myc, 3T3/E2F1, Saos-2/c-Myc, and Saos-2/E2F1. As shown in Figure 1A, the expression levels of c-Myc and E2F1 increased by ~2- to 3-fold in the corresponding transfectants. Under normal culture conditions, 3T3/c-Myc

and 3T3/E2F1 grew faster than mock-transfected 3T3/Mock (Figure 1B). When serum was removed, the total number of viable cells decreased more rapidly in 3T3/c-Myc and 3T3/E2F1 than in 3T3/Mock (Figure 1B). In DNA content analysis, the sub-G1 fraction formed from apoptotic cells emerged more prominently in 3T3/c-Myc and 3T3/E2F1 than in 3T3/Mock after serum depletion (Figure 1C). Similarly, serum deprivation evoked more severe apoptosis in Saos-2/c-Myc and Saos-2/E2F1 than in Saos-2/Mock (Figures 1B and 1C). Because Saos-2 lacks functional p53, both c-Myc and E2F1 were supposed to potentiate serum-deprived apoptosis independently of p53. Similar results were obtained from at least five independent clones in each transfectant (data not shown).

Apoptosis Cascades Are Activated More Rapidly in 3T3/c-Myc and 3T3/E2F1 than in 3T3/Mock

Next, we examined changes of $\Delta\Psi m$ during serum depletion by flow cytometry. In this method, the cells with disrupted $\Delta\Psi m$ are detected in the lower right area. After 24 hr serum starvation, $\Delta\Psi m$ decreased in a small proportion of 3T3/Mock, while it decreased in a substantial fraction of 3T3/c-Myc and 3T3/E2F1 (Figure 1D). Reflecting the decrease of $\Delta\Psi m$, more cytochrome c was released into cytoplasm in 3T3/c-Myc and 3T3/E2F1 than in 3T3/Mock (Figure 1E). Also, the cleavage (i.e., activation) of procaspase 3 occurred more rapidly (as early as 24 hr) in 3T3/c-Myc than in 3T3/Mock (Figure 1F). These results indicate that serum depletion activates common apoptosis cascades more rapidly in 3T3/c-Myc and 3T3/E2F1 than in 3T3/Mock.

c-Myc and E2F1 Induce ROS Accumulation in NIH3T3 and Saos-2

As Bcl-2 family proteins play a critical role in the regulation of $\Delta\Psi m$, we examined their mitochondrial localization in 3T3/Mock, 3T3/c-Myc, and 3T3/E2F1 before and after serum depletion. After 24 hr serum depletion, the amounts of mitochordrial Bcl-2 decreased; however, there was no significant difference among these clones (data not shown). Also, we did not detect an apparent change in the expression levels of Mcl-1 or Bax in these clones during serum depletion (data not shown). Since $\Delta\Psi m$ is also regulated by ROS (Adler et al., 1999; Cai et al., 1998), we examined ROS accumulation with a fluorescent sensor Red CC-1, which detects total ROS including superoxide anions, H_2O_2, organic peroxides, and hydroxyl radicals by flow cytometry. After 12 hr serum depletion, a small amount of ROS accumulated in 3T3/Mock (Figure 2A). By contrast, ROS were already present in 3T3/c-Myc and 3T3/E2F1 even under the culture with serum, which further increased after serum depletion (Figure 2A). Also, ROS accumulated more prominently in Saos-2/c-Myc and Saos-2/E2F1 than in Saos-2/Mock both before and after serum depletion (Figure 2A). The equivalent levels of ROS were detected in at least five independent clones of each transfectant before and after serum depletion (data not shown). To investigate the time course of ROS accumulation, we introduced 4-hydroxy-tamoxifen (4-HT)-inducible c-Myc, c-MycERT (a chimera consisting of c-Myc and estrogen receptor reactive to 4-HT), into NIH3T3 (this clone was named 3T3/c-MycERT). Even in the presence of serum, the 4-HT treatment evoked ROS accumulation in 3T3/c-MycERT from 4 to 12 hr (Figure 2B). To determine which types of ROS accumulated, we utilized dihydroethidium, which is specific for superoxide anions and chloromethyl-2′,7′-dichlorodihydrofluorescein diacetate (CM-H2DCFDA), which has been used to monitor H_2O_2 levels (Huang, et al. 2000; Sawada et al., 2001). As shown in Figure 2C, both superoxide anions and H_2O_2 are detected more abundantly in 3T3/c-Myc and 3T3/E2F1 than in 3T3/Mock before and after serum depletion, indicating that at least these two types of ROS are accumulated by c-Myc and E2F1.

c-Myc and E2F1 Sensitize NIH3T3 to Serum-Deprived Apoptosis through ROS

To assess the biologic function of ROS in serum-deprived apoptosis, we overexpressed MnSOD in 3T3/c-Myc and 3T3/E2F1; each clone was designated 3T3/c-Myc/MnSOD and 3T3/E2F1/MnSOD. We examined the effects of MnSOD and the catalase treatment on ROS accumulation, $\Delta\Psi m$, and nuclear fragmentation by confocal microscopy (Figure 2D). Although the accumulation of ROS (detected as red fluorescence) and the decrease of $\Delta\Psi m$ (detected as green fluorescence) were provoked by serum depletion in catalase-untreated 3T3/c-Myc and 3T3/E2F1, these changes were abolished in catalase-treated 3T3/c-Myc, 3T3/c-Myc/MnSOD, and 3T3/E2F1/MnSOD. As a result, nuclear fragmentation was significantly inhibited in these clones as compared with catalase-untreated 3T3/c-Myc and 3T3/E2F1. Consistent with these data, overexpression of MnSOD or the catalase treatment reduced the sub-G1 fraction in 3T3/c-Myc and 3T3/E2F1 in flow cytometric analysis (Figure 2E). In addition, another antioxidant, N-acetylcysteine, reduced E2F1- or c-Myc-enhanced serum-deprived apoptosis as efficiently as catalase (data not shown). These results suggest that ROS may be involved in c-Myc- and E2F1-mediated apoptosis.

Serum Depletion Induces MnSOD mRNA in 3T3/Mock but Not in 3T3/c-Myc or 3T3/E2F1

Next, we examined changes in mRNA expression of MnSOD and Cu/ZnSOD that play a crucial role in ROS elimination (Figure 3A). The expression of MnSOD mRNA was hardly detectable in all clones under the culture with serum (0 hr). However, its expression was induced by serum depletion in 3T3/Mock, but not in 3T3/c-Myc or 3T3/E2F1. Also, the 4-HT-activated c-Myc abrogated its induction in 3T3/c-MycERT. In contrast, the expression of Cu/ZnSOD mRNA did not change during serum starvation in these clones. Also, we did not detect an apparent difference in its expression levels among these clones. In agreement with these data, serum depletion induced MnSOD activity in 3T3/Mock but not in 3T3/c-Myc or 3T3/E2F1 (Figure 3B). These results suggest that overexpressed c-Myc and E2F1 may promote ROS accumulation and consequent apoptosis by inhibiting MnSOD induction during serum deprivation.

Serum Depletion Activates MnSOD Promoter through ROS-Activated NF-κB

We analyzed the mechanism of MnSOD induction during serum depletion. In 3T3/Mock, both actinomycin D and

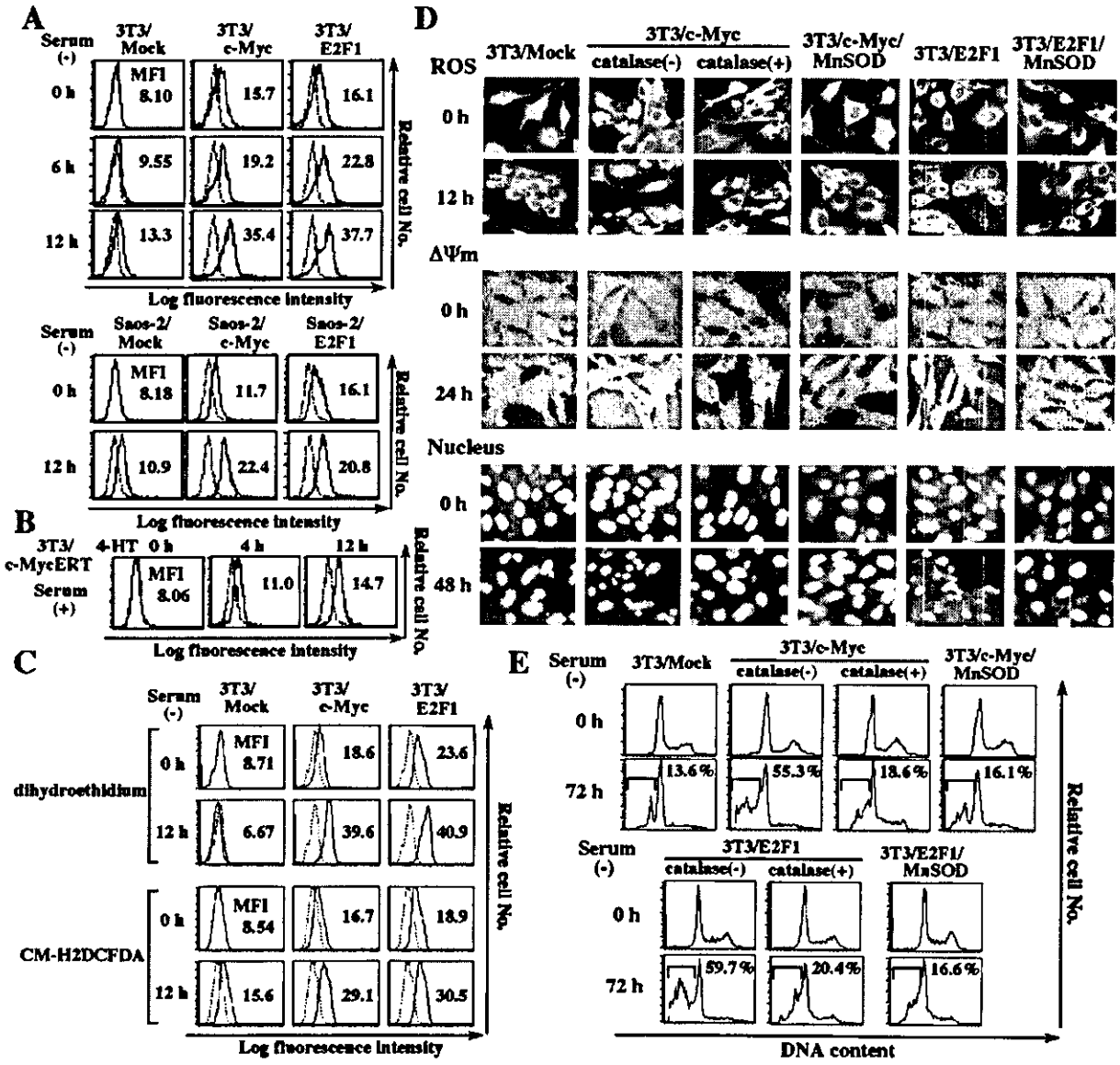

Figure 2. Biologic Function of ROS in c-Myc- and E2F1-Enhanced Apoptosis

(A and B) The cells were deprived of serum or treated with 1 μM of 4-hydroxytamoxifen (4-HT) for the time indicated. Total ROS were detected with Red CC-1 by flow cytometry. Mean fluorescent intensity (MFI) is indicated.

(C) Superoxide anions were detected with dihydroethidium and H_2O_2 with CM-H2DCFDA.

(D) The cells were deprived of serum in the presence or absence of catalase (50 U/ml). ROS were detected with Red CC-1 and the decrease of ΔΨm with DePsioher by fluorescence microscopy. Nuclei were visualized with Hoechst 33342.

(E) DNA content of the cultured cells was examined by PI staining. The proportion of the sub-G1 fraction is indicated.

cycloheximide inhibited MnSOD expression induced by serum depletion (data not shown), suggesting that this induction requires RNA synthesis and protein synthesis and is regulated at a transcriptional level. So, we performed luciferase assays with −2505-SOD-Luc containing −2505 bp of the MnSOD promoter and its deletion mutants (Figure 3C). In 3T3/Mock, serum depletion activated −2505-, −1460-, −1104-, and −360-SOD-Luc but not −345-SOD-Luc (Figure 3D), suggesting that serum depletion may activate MnSOD promoter through a putative NF-κB binding site at −350 bp (named SOD-κB-2). As an additional NF-κB binding site was found at −1420 bp (named SOD-κB-1), we introduced mutations at SOD-κB-1 and/or SOD-κB-2 into −1460-SOD-Luc to generate −1460-κB-1m-Luc, −1460-κB-2m-Luc, and −1460-κB-1,2m-Luc. Although −1460-κB-1m-Luc and −1460-κB-2m-Luc were still activated by serum depletion, either mutation equally reduced the response from 3.5- to 1.8-fold in these reporter genes (Figure 3D). In addition, −1460-SOD-κB-1,2m-Luc scarcely reacted to serum depletion (by 1.1-fold). We also constructed reporter genes, each containing three tandem repeats of (3×) SOD-κB-1, SOD-κB-2, mutated SOD-κB-1 (SOD-κB-1m), and mutated SOD-κB-2 (SOD-κB-2m) in front of the thymidine kinase minimal promoter. As shown in Figure 3E, 3×SOD-κB-1-Luc and 3×SOD-κB-2-Luc but

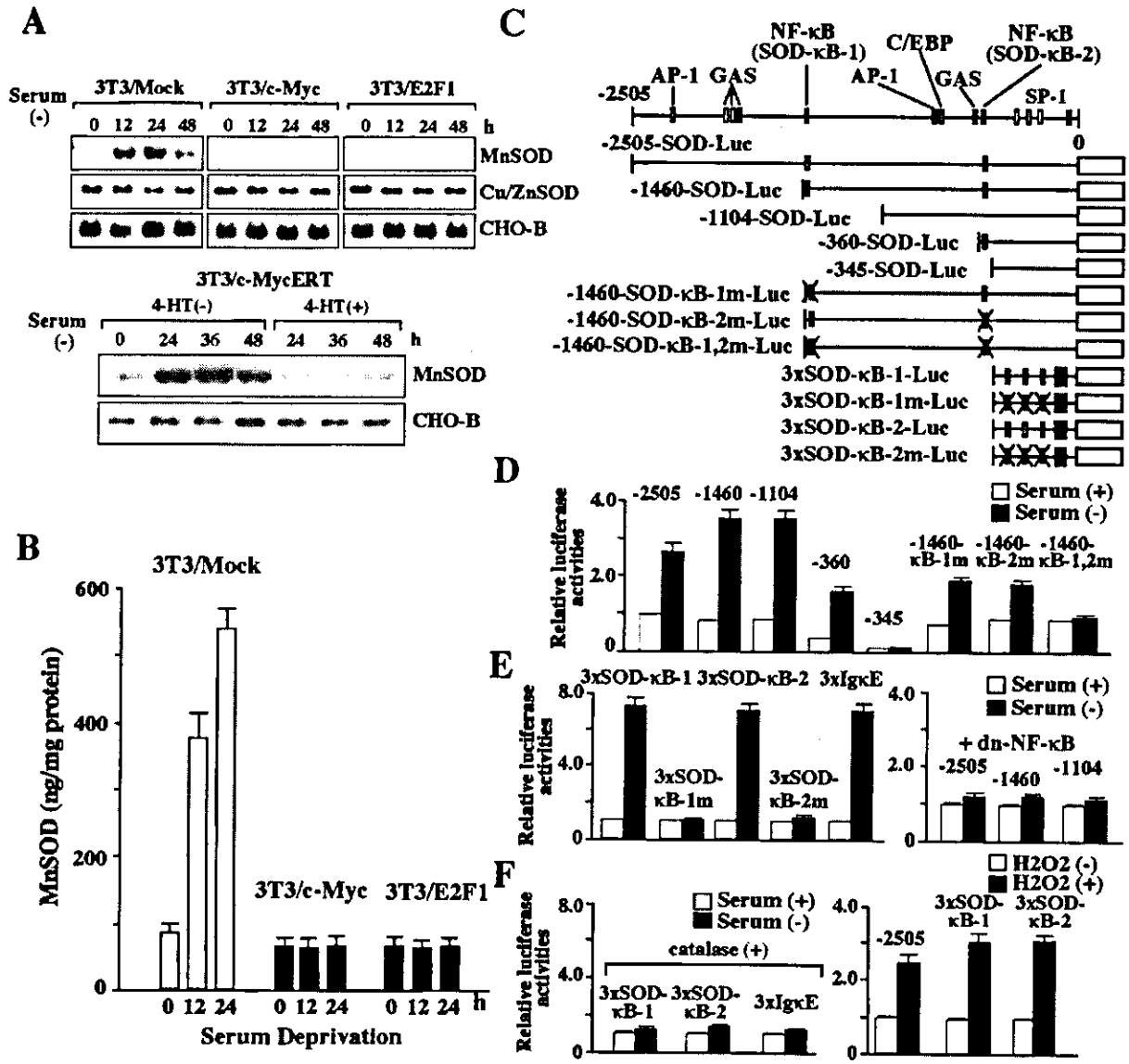

Figure 3. Regulation of MnSOD Promoter Activity during Serum Depletion

(A) The cells were deprived of serum, and cultured with or without 1 μM of 4-HT for the time indicated and subjected to Northern blot analysis.
(B) Mitochondrial MnSOD activity was measured by ELISA. The results are shown as the mean ± SD of triplicate measurement.
(C) Structure of MnSOD luciferase reporter genes.
(D and E) 3T3/Mock cells seeded in 60 mm dish were transfected with 2 μg of the indicated reporter gene and 10 ng of pRL-CMV-Rluc by the calcium phosphate coprecipitation method. As an effector gene, 8 μg of an expression vector for dominant negative (dn) NF-κB was cotransfected with the reporter gene in the indicated experiments ([E], right panel). After 12 hr, the cells were cultured with or without serum for 24 hr and then subjected to luciferase assays. The results are shown as the mean ± SD of triplicate cultures.
(F) 12 hr after the transfection, the cells were cultured with 50 U/ml of catalase in the presence or absence of serum for 24 hr (left panel) or cultured with serum for 24 hr followed by the 6 hr stimulation with 200 μM of H_2O_2 (right panel). Then, these cells were subjected to luciferase assays.

not 3×SOD-κB-1m-Luc or 3×SOD-κB-2m-Luc were activated by serum depletion as efficiently as 3×IgκE-Luc containing 3× typical NF-κB binding sequence of the immunoglobulin κ enhancer (IgκE). Furthermore, dominant-negative (dn) NF-κB inhibited serum-depletion-induced −2505-, −1460- and −1104-SOD-Luc activities (Figure 3E). These results imply that serum depletion activates NF-κB and induces MnSOD promoter activity through both SOD-κB-1 and SOD-κB-2 sites. However, the fold increase in −2505-SOD-Luc (~3- to 4-fold) was lower than that in the protein levels in Figure 3B (~6- to 7-fold). Regarding this discrepancy, it was reported that, in addition to SOD-κB-1 and SOD-κB-2, there is another NF-κB binding site in the intron 2 of the murine MnSOD gene, which contributes to TNF-α-induced MnSOD promoter activity (Jones et al., 1997). Thus, this intronic NF-κB site was supposed to be also required for ROS-induced full activation of MnSOD promoter.

To elucidate the mechanism of NF-κB activation during serum depletion, we examined the effects of ROS

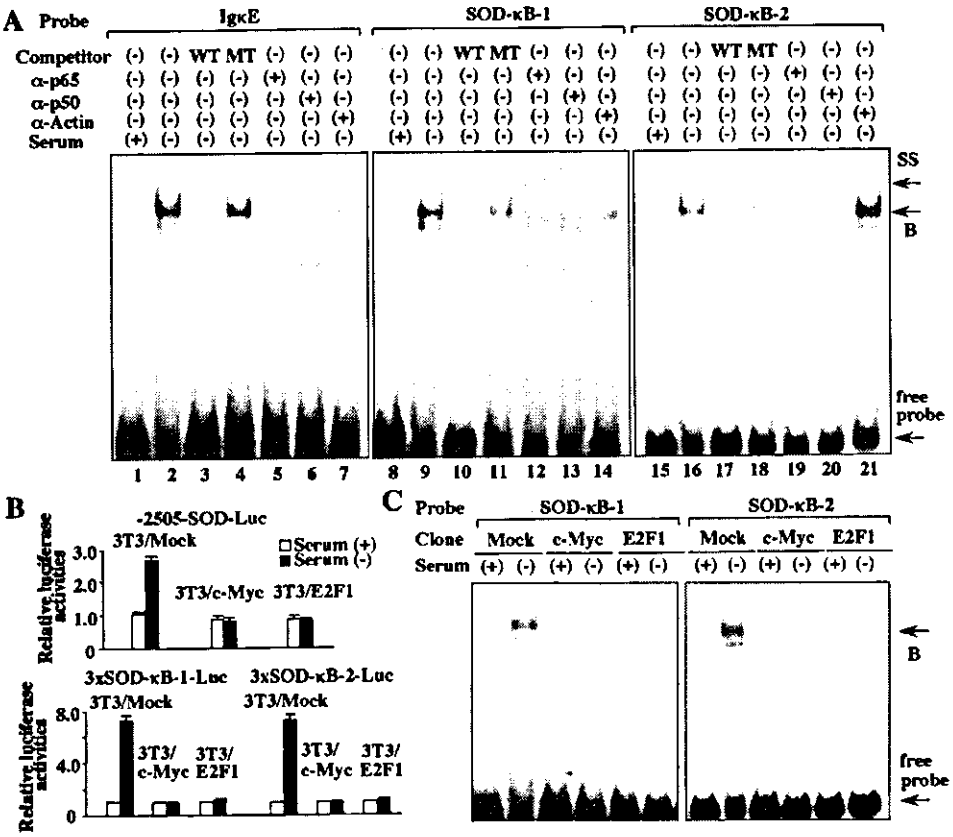

Figure 4. Inhibition of DNA Binding Activity of NF-κB by c-Myc and E2F1

(A) Nuclear extracts were isolated from 3T3/Mock before and after 24 hr serum depletion and subjected to EMSA. In competition assays, a 200-fold M excess of unlabeled competitor oligonucleotide was added to the binding mixture. In supershift assays, nuclear extracts were preincubated with 1 μg of the indicated Ab prior to the binding reaction. B, DNA binding complex; SS, supershifted complex.

(B) The cells were transfected with the indicated reporter gene, cultured with or without serum for 24 hr, and then subjected to luciferase assays.

(C) Nuclear extracts were prepared from 3T3/Mock, 3T3/c-Myc, and 3T3/E2F1 before and after 24 hr serum starvation. DNA binding activity of NF-κB was examined with the probes of SOD-κB-1 and SOD-κB-2.

on NF-κB activity in 3T3/Mock because ROS were reported to activate NF-κB in other cell types (Rhee, 1999). When ROS were eliminated by the catalase treatment, serum depletion did not activate 3×SOD-κB-1-Luc, 3×SOD-κB-2-Luc, or 3×IgκE-Luc (Figure 3F). Moreover, H_2O_2-produced ROS activated −2505-SOD-Luc, 3×SOD-κB-1-Luc, and 3×SOD-κB-2-Luc (Figure 3F), suggesting that ROS would activate NF-κB during serum deprivation.

Overexpressed c-Myc and E2F1 Inhibit DNA Binding Activity of NF-κB

Next, we performed electropholic mobility shift assay (EMSA) with the probes of IgκE, SOD-κB-1, and SOD-κB-2 (Figure 4A). The nuclear extract isolated from 3T3/Mock after serum depletion bound to these probes (lanes 2, 9, and 16). These complexes were abolished by the wt competitor (lanes 3, 10, and 17) but not by the mutant (MT) competitor (lanes 4, 11, and 18). Although the control Ab (an anti-actin Ab) reduced (lanes 7 and 14) or augmented (lane 21) the amounts of the complex, it did not yield the supershifted band. In contrast, these complexes were supershifted by the anti-p65 Ab (lanes 5, 12, and 19) and the anti-p50 Ab (lanes 6, 13, and 20), implying that these complexes contain NF-κB.

Because serum starvation did not induce MnSOD mRNA in 3T3/c-Myc and 3T3/E2F1 (Figure 3A), we performed luciferase assays in these clones. In contrast to 3T3/Mock, serum depletion failed to activate -2505-SOD-Luc, 3×SOD-κB-1-Luc, and 3×SOD-κB-2-Luc in 3T3/c-Myc and 3T3/E2F1, suggesting that MnSOD is not induced due to the defect of NF-κB activation in these clones (Figure 4B). Supporting these findings, the nuclear extracts obtained from 3T3/c-Myc and 3T3/E2F1 after serum depletion scarcely bound to SOD-κB-1 and SOD-κB-2, indicating that DNA binding activity of NF-κB is impaired in these clones (Figure 4C).

E2F1 but Not c-Myc Binds to p65 and Inhibits NF-κB Activity

Since ROS-induced NF-κB activity was impaired in both 3T3/c-Myc and 3T3/E2F1, we examined the relationship between these clones. As shown in Figure 5A, the expression of c-Myc in 3T3/E2F1 increased to the levels comparable to that in 3T3/c-Myc. Also, the expression

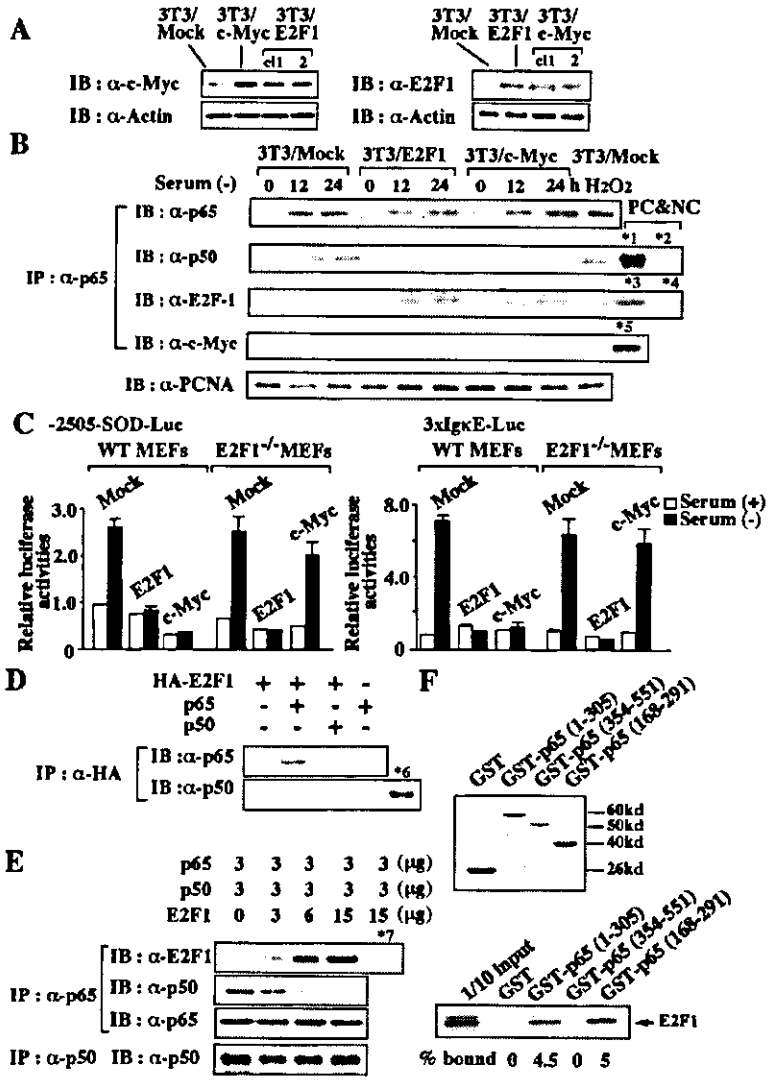

Figure 5. The Competition between E2F1 and p50 in the Binding to p65

(A) The expression of c-Myc and E2F1 was examined in 3T3/c-Myc and 3T3/E2F1 by immunoblot analysis.

(B) The cells were deprived of serum and nuclear lysates were prepared at the time indicated. The in vivo binding among p65, p50, E2F1, and c-Myc was examined by coimmunoprecipitation analyses. PC, positive control; NC, negative control; *1, anti-p50 immunoprecipitation (IP) from serum-deprived 3T3/Mock; *2, anti-actin IP from serum-deprived 3T3/Mock; *3, anti-E2F1 IP with an KH95 Ab from serum-deprived 3T3/E2F1; *4, anti-actin IP from serum-deprived 3T3/E2F1; *5, anti-c-Myc IP from 3T3/c-Myc.

(C) wt and E2F1$^{-/-}$ MEFs were transfected with 2 μg of −2505-SOD-Luc or 3×IgκE-Luc together with 8 μg of the expression vector indicated. After 12 hr, the cells were cultured with or without serum for 24 hr and subjected to luciferase assays.

(D and E) 293T cells were transfected with expression vectors for p65, p50, and HA-tagged E2F1 in various combinations as indicated. The relationship among E2F1, p65, and p50 in the heterodimer formation was examined by coimmunoprecipitation analyses. *6, anti-p50 IP from p50-transfected 293T; *7, anti-actin IP.

(F) The quality and quantity of purified GST-p65 proteins were confirmed by coommassie blue staining (upper panel). The in vitro binding between ^{35}S-labeled E2F1 and various types of GST-p65 was examined by a GST-pull-down experiment (lower panel).

of E2F-1 increased in 3T3/c-Myc as well as in 3T3/E2F1. These results indicate that E2F1 augments the expression of c-Myc in NIH3T3 and vise versa.

Next, we analyzed the influence of c-Myc and E2F1 on the dimer formation between NF-κB subunits p65 and p50 with nuclear extracts isolated from 3T3/Mock, 3T3/c-Myc, and 3T3/E2F1. As a positive control for nuclear protein containing active NF-κB, we utilized the nuclear extract isolated from H_2O_2-stimulated 3T3/Mock. At first, we performed immunoblotting with an anti-PCNA Ab and confirmed that equal amounts of nuclear extracts were isolated (Figure 5B). Also, we verified that these nuclear preps were not contaminated by cytosolic protein with immunoblot analysis using an anti-actin Ab (actin which exclusively exists in the cytosol was not detected in any lysates) (data not shown). As shown in Figure 5B, the anti-p65 immunoblot on the anti-p65 immunoprecipitated proteins showed that p65 is translocated to the nucleus in 3T3/Mock, 3T3/E2F1, and 3T3/c-Myc during serum depletion. Importantly, the amount of p50 coimmunoprecipitated with p65 increased after serum depletion in 3T3/Mock, but not in 3T3/E2F1 or 3T3/c-Myc. By contrast, the equivalent amount of E2F1 was coimmunoprecipitated with p65 instead of p50 in 3T3/E2F1 and 3T3/c-Myc after serum depletion (Figure 5B). However, we did not detect the binding between c-Myc and p65 in any clones. These results suggest that E2F1 but not c-Myc may directly suppress NF-κB activity by inhibiting the p65/p50 dimer formation in 3T3/c-Myc and 3T3/E2F1.

To further examine the roles of c-Myc and E2F1 in the inhibition of NF-κB activity, we performed luciferase assays with −2505-SOD-Luc and 3×IgκE-Luc in wt and E2F1$^{-/-}$ murine embryonic fibloblasts (MEFs) (Figure 5C). As expected, serum depletion activated both reporter genes in wt and E2F1$^{-/-}$ MEFs, and cotransfected E2F1 inhibited this induction in both MEFs. Furthermore, it was of importance to note that cotransfected c-Myc inhibited this induction in wt MEFs, but not in E2F1$^{-/-}$ MEFs, providing evidence that c-Myc inhibits NF-κB activity through E2F1.

E2F1 and p50 Competitively Bind to p65

In a previous paper, E2F1 was shown to suppress TNF-α-induced NF-κB activity by inhibiting IKK activation (Phillips et al., 1999). However, we found that serum

depletion activated IKK (data not shown) and that activated NF-κB was translocated to the nucleus in 3T3/E2F1 (Figure 5B). These results indicate that E2F1 would inhibit NF-κB activity through the different mechanism in NIH3T3.

To examine the relationship between p65/p50 and E2F1 in the complex formation, we transfected HA-tagged E2F1, p65, and/or p50 into 293T cells and found that p65, but not p50, was coimmunoprecipitated with E2F1 (Figure 5D). Next, we transfected p65 and p50 with various doses of E2F1. As shown in Figure 5E, the amounts of E2F1 coimmunoprecipitated with p65 increased dependently on the doses of E2F1. In contrast, the amounts of p50 coimmunoprecipitated with p65 decreased as the binding between p65 and E2F1 increases, implying that E2F1 binds to p65 in competition with p50 and inhibits the formation of functional NF-κB, p65/p50. Furthermore, we found that ^{35}S-labeled E2F1 bound to GST-p65 (1–305), but not to GST alone or GST-p65 (354–551) (Figure 5F). Supporting the hypothesis that E2F1 and p50 competitively bind to p65, E2F1 bound to GST-p65 (168–291) containing the p50 binding domain.

E2F1 Inhibits NF-κB Activity through Both DP-1 Binding Domain and DNA Binding Domain

To determine which domain of E2F1 inhibits NF-κB activity, we transfected −2505-SOD-Luc together with each mutant E2F1 into NIH3T3 and performed luciferase assays (Figure 6A). Δ1-88, Δ113-120, and 411/421 inhibited serum-depletion-induced NF-κB activity as efficiently as wt E2F1. In contrast, E132, Δ206-220, Δ123-437, or Δ192-437 could not inhibit NF-κB activity, suggesting that E2F1 inhibits NF-κB activity through both DNA binding domain and DP-1 binding domain. Supporting this hypothesis, mutant E2F1 consisting of only these two domains (122-243) could suppress NF-κB activity, whereas 122-243 harboring E132 (122-243/E132) was hardly effective. In addition, p65 bound to wt E2F1, Δ1-88, and 122-243, but not to E132 or Δ206-220 in the coimmunoprecipitation experiment (Figure 6B), indicating that both domains of E2F1 are required and sufficient for this binding.

To assess biologic function of 122-243 in serum-deprived apoptosis of NIH3T3, we performed a transient transfection experiment because we could not prepare a stable clone overexpressing 122-243. For this reason, we speculated that 122-243, which reveals the structual similarity to E2F6, would act as a dn mutant over endogenous E2Fs. To distinguish the cells transfected with the effector gene, we cotransfected an expression vector of red fluorescent protein (DsRed) and detected apoptotic cells with Annexin-V-EGFP by fluorescent microscopy. After 48 hr serum deprivation, NIH3T3 cells transfected with an empty vector (Mock) or 122-243/E132 were still negative for Annexin-V, while most (over 90%) of the cells transfected with wt E2F1 or 122-243 were positive for Annexin-V (Figure 6C). These data indicate that 122-243 enhances serum-deprived apoptosis as efficiently as wt E2F1.

We also examined the effects of other E2F members and DP-1 on NF-κB activity. As compared with E2F1, E2F2-4 showed little inhibitory effect on NF-κB activity (Figure 6D). In addition, it was of interest that DP-1 recovered NF-κB activity suppressed by E2F1, whereas DP-1 by itself did not affect NF-κB activity. This result suggests that E2F1, which is in a complex with DP-1, cannot suppress NF-κB activity.

Endogenous E2F1 Also Inhibits NF-κB Activity

We next analyzed the effects of endogenous E2F1 on NF-κB activity. We transfected the FITC-labeled antisense (AS) oligonucleotide against E2F1 into NIH3T3 by lipofection and sorted the cells with strong FITC intensities (Figure 7A, left panel). Similarly, we sorted the cells each transfected with the sense (S)-E2F1 and the mismatched (MM) oligonucleotides (data not shown). In sorted cells, AS-E2F1 reduced the amount of endogenous E2F1 almost completely (over 95%), while S-E2F1 and MM scarcely affected its amount (Figure 7A, middle panel). Under these conditions, H_2O_2 activated NF-κB more effectively in AS-E2F1-transfected cells than in S-E2F1- or MM-transfected cells (Figure 7A, right panel), suggesting that endogenous E2F1 may inhibit NF-κB activity. To further explore the effects of endogenous E2F1 on NF-κB activity, we synchronized NIH3T3 cells at G1 phase by serum depletion. After addition of serum, cell cycle synchronously progressed to G1/S boundary at 12 hr, S phase at 18 hr, and G2/M phase at 24 hr (Figure 7B, left panel). We stimulated the cells with H_2O_2 at each time point and performed luciferase assays. When DP-1 was not transfected, H_2O_2 activated NF-κB with various efficiencies dependently on the phase of cell cycle: 3.7-fold at G1; 1.3-fold at G1/S; 1.5-fold at S; 3.3-fold at G2/M; and 2.1-fold in nonsynchronized (NS) cells (Figure 7B, right panel). In contrast, when DP-1 was transfected, H_2O_2 activated NF-κB with constant high efficiencies (by about 4-fold) irrespective of the phase of cell cycle (Figure 7B, right panel). We performed the same analyses on wt and E2F1$^{-/-}$ MEFs. After 48 hr serum depletion, serum was added to the culture medium. As shown in Figures 7C and 7D (left panels), cell cycles progressed with the similar pace in wt and E2F1$^{-/-}$ MEFs (G1/S at 12 hr, S at 18 hr, and G2/M at 24 hr). As was the case with NIH3T3, H_2O_2 activated NF-κB with various efficiencies according to the phase of cell cycle in wt MEFs (2.4-fold at G1; 1.1-fold at G1/S; 1.1-fold at S; 2.2-fold at G2/M; or 1.8-fold in NS), while cotransfected DP-1 cancelled this cell cycle-dependent change of NF-κB activities (Figure 7C, right panel). In contrast, H_2O_2-induced NF-κB activities were kept constant (about 3-fold induction) regardless of cell cycle in E2F1$^{-/-}$ MEFs (Figure 7D, right panel). Also, cotransfected DP-1 hardly affected its activities in E2F1$^{-/-}$ MEFs (Figure 7D, right panel). Moreover, when E2F1 was introduced into E2F1$^{-/-}$ MEFs, H_2O_2-induced NF-κB activity was dose-dependently suppressed by E2F1 in these cells, which was also restored by cotransfected DP-1 (data not shown). Together, these data imply that endogenous E2F1 inhibits NF-κB activity in a cell cycle-dependent manner (i.e., only when it is released from Rb) and that excessive DP-1 would sequester E2F1 from p65 and contribute to the reconstitution of functional NF-κB (as summarized in Figure 7E).

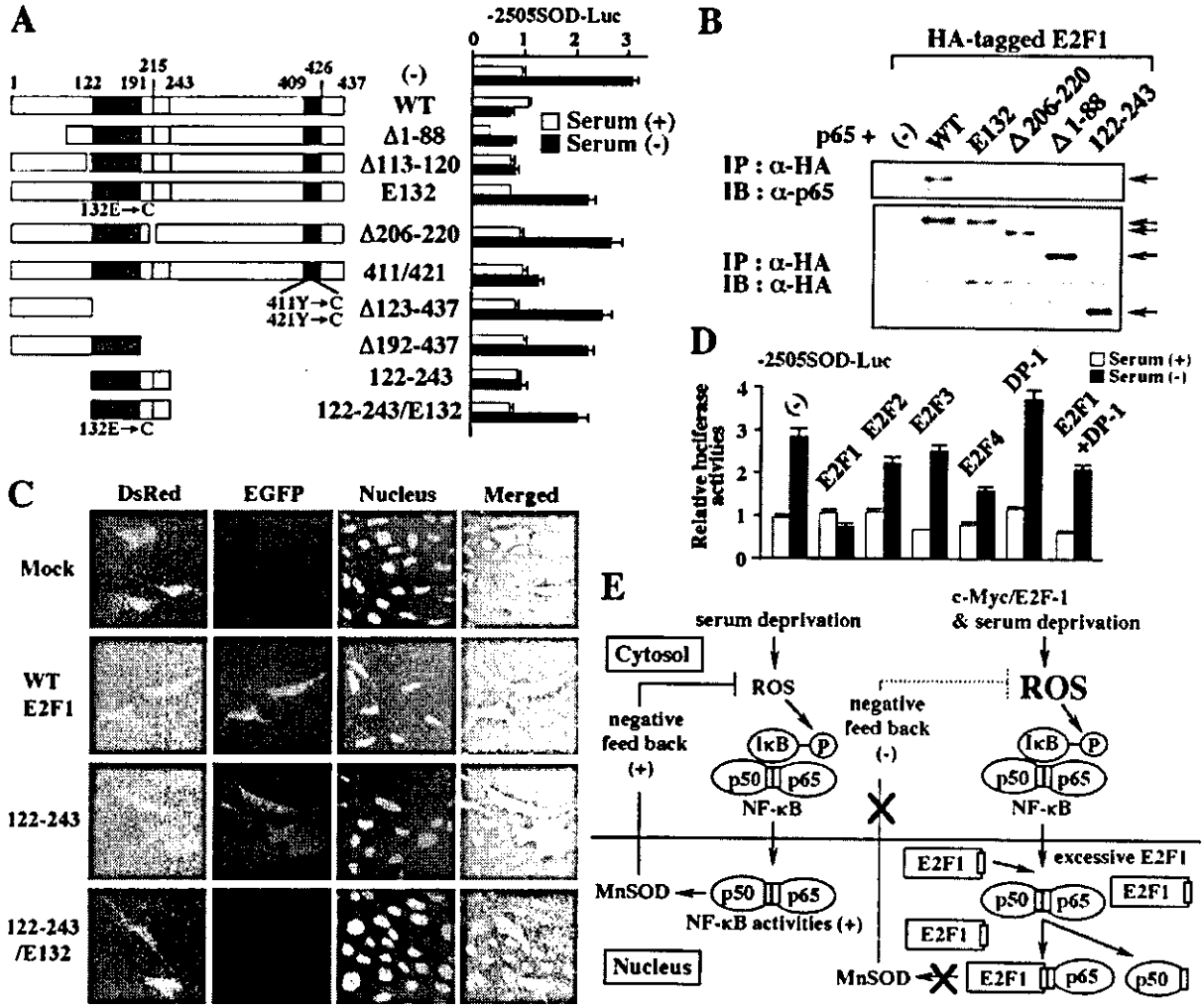

Figure 6. Domains of E2F1 that Inhibit NF-κB Activity

(A) Structure of mutant E2F1s. Hatched, DNA binding domain; dotted, DP-1 binding domain; black, Rb binding domain. NIH3T3 cells were transfected with 2 μg of −2505SOD-Luc together with 8 μg of wt or mutant E2F1 as indicated. After 12 hr, the cells were washed, cultured with or without serum for 24 hr, and subjected to luciferase assays.

(B) 293T cells were transfected with p65 and HA-tagged wt or mutant E2F1 as indicated. The in vivo binding between p65 and mutant E2F1 was examined by the coimmunoprecipitation method. The lower panel indicates that each mutant E2F1 protein was effectively produced in 293T cells.

(C) NIH3T3 cells were transfected with 1 μg of an expression vector of Discosoma sp red fluorescent protein (DsRed) and 10 μg of the effector gene indicated. After 48 hr serum depletion, apoptotic cells were detected with Annexin-V-EGFP by fluorescent microscopy. Nuclei were visualized with Hoechst 33342.

(D) NIH3T3 cells were transfected with 2 μg of −2505SOD-Luc together with 8 μg of effector gene(s) (E2F1-4 and/or DP-1). After 12 hr, the cells were washed, cultured with or without serum for 24 hr, and subjected to luciferase assays.

(E) A possible model of E2F1-enhanced serum-deprived apoptosis. In normal cells, serum starvation leads to ROS accumulation. Accumulated ROS, in turn, activate NF-κB and induce MnSOD expression, which eliminates ROS as a negative feedback regulator. In contrast, ROS are already accumulated in the cells overexpressing E2F1 or c-Myc even under proliferative conditions. After serum deprivation, the amount of ROS further increases in these cells. Although ROS-activated NF-κB is translocated to the nucleus, excessive E2F1, which is not in a complex with DP-1, inhibits its activity by binding to p65, thereby suppressing MnSOD induction. Because ROS are not eliminated by MnSOD, these cells are more susceptible to serum-deprived apoptosis.

Discussion

Roles for E2F1 in c-Myc-Induced Apoptosis

Leone and colleagues recently reported that c-Myc-induced apoptosis was severely reduced in E2F1$^{-/-}$ MEFs (Leone et al., 2001). Regarding this mechanism, we here showed that c-Myc augments the expression of E2F1 in NIH3T3 and that E2F1 inhibits NF-κB activity in both 3T3/E2F1 and 3T3/c-Myc. In addition, we found that c-Myc inhibits ROS-induced NF-κB activity through

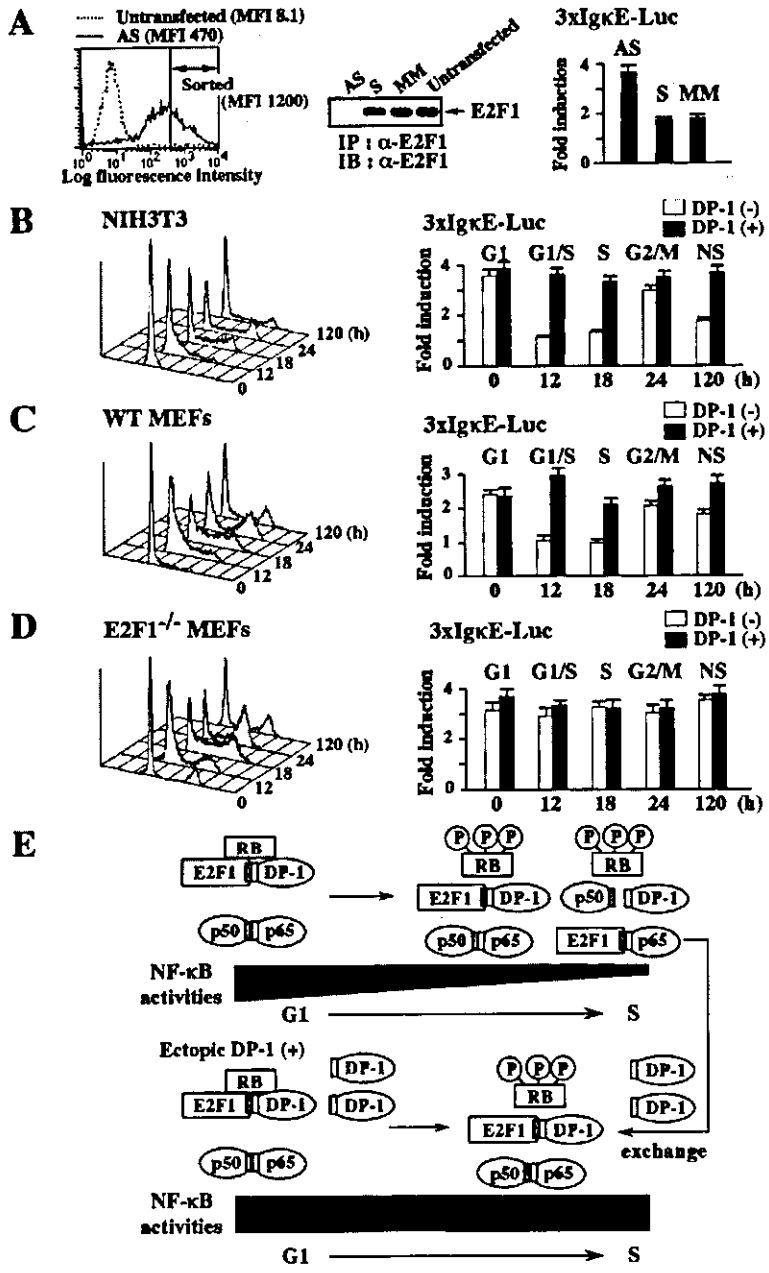

Figure 7. Effects of Endogenous E2F1 on NF-κB Activity

(A) NIH3T3 cells were transfected with 12 μg of each FITC-labeled oligonucleotide and 0.5 μg of 3×IgGκE-Luc by lipofection. After 24 hr, the cells with strong FITC intensity were sorted by FACS vantage (left panel) and cultured with serum for 12 hr. The amounts of E2F1 in the cultured cells were examined by immunoblot analysis (middle panel). Another aliquot of the cultured cells was stimulated with 200 μM of H_2O_2 for 6 hr and subjected to luciferase assays (right panel). AS, antisense; S, sense; MM, mismatched control.

(B–D) NIH3T3, wt MEFs, and E2F1$^{-/-}$ MEFs were transfected with 0.5 μg of 3×IgGκE-Luc with or without 8 μg of an expression vector for DP-1 and synchronized at G1 phase by serum depletion. Then, serum was added, and the cultured cells were subjected to cell cycle analysis at the time indicated (left panel). Also, another aliquot of the cultured cells was stimulated with 200 μM of H_2O_2 for 6 hr and subjected to luciferase assays (right panel). NS, nonsynchronized.

(E) A possible model of cell cycle-dependent inhibition of NF-κB activity by E2F1. E2F1 captured by Rb cannot inhibit NF-κB activity at G1 phase. When released from Rb during cell cycle progression from G1 to S phase, a significant proportion of E2F1 would form a complex with p65, thereby inhibiting NF-κB activity around S phase. However, when DP-1 is ectopically expressed, excessive DP-1 would sequester E2F1 from p65 and contribute to the reconstitution of functional NF-κB.

E2F1 by using E2F1$^{-/-}$ MEFs. These data indicate that E2F1 may play a critical role in c-Myc-enhanced apoptosis by inhibiting NF-κB activity.

E2F1 Enhances Apoptosis through Several Mechanisms

c-Myc and E2F1 were reported to stabilize p53 through the induction of ARF, which inhibits MDM2-mediated degradation of p53, and to cause apoptosis in a p53-dependent manner (Zindy et al., 1998; Bates et al., 1998). However, E2F1 also induces apoptosis via p53-independent pathways, whereas p53-dependent pathways indeed augment this apoptosis (Phillips et al., 1999; Hsieh et al., 1997). Moreover, in this study, c-Myc and E2F1 enhanced serum-deprived apoptosis in ARF null NIH3T3 and in p53-defective Saos-2. As for this inconsistency, E2F1 was reported to induce the expression of the p53 homolog p73, which plays a central role in E2F1-induced apoptosis of p53$^{-/-}$ MEFs and T cell receptor-activation-induced apoptosis of T cells (Irwin et al., 2000; Lissy et al., 2000). Furthermore, E2F1 was shown to induce proapoptotic molecules, caspase-3 and Apaf-1 (Muller et al., 2001; Moroni, et al., 2001). These lines of evidence suggest that E2F1 would potentiate apoptosis as a transcription factor. In contrast, it was also reported that mutant E2F1 lacking transcriptional activity could enhance apoptosis as efficiently as wt E2F1 (Phillips et al., 1999; Hsieh et al., 1997). Moreover, in this study, mutant E2F1 122-243, which lacks transcriptional activity but can inhibit NF-κB activity, enhanced serum-deprived

apoptosis as efficiently as wt E2F1. Thus, E2F1 was supposed to augment serum-deprived apoptosis by inhibiting NF-κB activity in NIH3T3.

We demonstrated that overexpression of DP-1 can recover NF-κB activity suppressed by E2F1. This result suggests that DP-1 may play some role as an antiapoptotic molecule by protecting NF-κB activity from E2F1. In addition to the E2F1/DP-1/p65 interaction, both E2F1 and DP-1 were shown to interact with p53 and to affect the amount and activity of p53 (Sorensen et al., 1996; Nip et al., 2001). So, the E2F1/DP-1 complex was considered to affect cell survival through the direct interaction with critical apoptosis regulatory molecules, NF-κB and p53. Together, these results suggest that E2F1 may potentiate apoptosis via totally different mechanisms through its transcriptional activity and/or the interaction with apoptosis regulatory molecules.

Endogenous E2F1 Inhibits NF-κB Activity and Enhances Apoptosis

We found that endogenous E2F1 released from Rb inhibits NF-κB activity as well as overexpressed E2F1. This result suggests that normally proliferating cells become susceptible to proapoptotic stimuli due to the lack of NF-κB activity every time they pass through S phase during cell cycle progression. In fact, apoptosis of thymic T cells was disrupted, and various types of tumors developed in E2F1$^{-/-}$ mice (Field et al., 1996; Yamasaki et al., 1996). Together, these results suggest that endogenous E2F1 would inhibit NF-κB activity and make various types of cells susceptible to apoptosis, thereby acting as a tumor suppressor.

Mechanisms of ROS Accumulation Induced by Excessive c-Myc or E2F1

ROS are mainly generated at mitochondrial electron transport chains during normal cellular metabolism. In addition, various stimuli, including TNF-α, Fas ligand, and growth factors, rapidly (as early as 1–20 min) provoke ROS accumulation in the target cells (Suzuki et al., 1998; Goldman et al., 1998). In contrast, NGF (nerve growth factor) depletion induces ROS accumulation in neuronal cells at a later phase (after 3–6 hr), which was inhibited by actinomycin D and cycloheximide (Greenlund et al., 1995), implying that mRNA synthesis and protein synthesis were necessary for this ROS accumulation. These results indicate that ROS are generated through different mechanisms according to the culture systems. Although p53 was reported to induce various ROS-producing genes (Polyak et al., 1997), in the present study, overexpression of c-Myc or E2F1 led to ROS accumulation in p53 null Saos-2, implying that ROS accumulate independently of p53 in this system. Although prominent ROS accumulation in 3T3/E2F1 and 3T3/c-Myc after serum depletion was attributable to the defect of MnSOD induction, 4-HT-induced c-Myc caused ROS accumulation in 3T3/c-MycERT cells that keep proliferating in the presence of serum with normal $\Delta\Psi m$ (data not shown), indicating that neither mitochondrial injury nor apoptosis is implicated in this ROS accumulation. Thus, it remains unclear how excessive c-Myc and E2F1 accumulate ROS in undamaged, proliferating cells.

Roles for ROS-Activated NF-κB in Serum-Deprived Apoptosis

ROS can induce apoptosis through activation of JNK (Benhar et al., 2001). Meanwhile, Phillips and colleagues reported that E2F1 inhibits TNF-α-induced JNK activity in Saos-2 (Phillips et al., 1999). So, we examined the activation state of JNK in 3T3/Mock and 3T3/E2F1 during serum depletion by immunoblot analysis with an anti-phospho-JNK Ab. However, JNK was activated in neither clone (data not shown). Also, dn JNK did not affect NF-κB activity or apoptosis induced by serum depletion in these clones (data not shown). Thus, it is not likely that JNK is involved in serum-deprived apoptosis of NIH3T3.

We showed that NF-κB activity was inhibited in 3T3/c-Myc and 3T3/E2F1. Besides MnSOD, the induction of other antiapoptotic target genes of NF-κB such as Bcl-XL, cIAP1, and cIAP2 were also suppressed in these clones (data not shown). However, overexpression of either molecule was less effective than that of MnSOD to cancel serum-deprived apoptosis in these clones (data not shown). So, we assumed that the defect of MnSOD induction and consequent ROS accumulation were the major causes of serum-deprived apoptosis in these clones (as summarized in Figure 6E). However, it is also possible that the lack of other target molecules of NF-κB might be more critical for different types of apoptosis in the cells overexpressing E2F1 or c-Myc.

NF-κB can also exhibit proapoptotic activity under different conditions (Barkett and Gilmore, 1999). For example, NF-κB mediates activation-induced apoptosis through the induction of Fas-ligand in T cells. NF-κB is indispensable for p53-induced apoptosis in Saos-2 (Ryan et al., 2000). Also, ROS-activated NF-κB plays an essential role in H_2O_2-induced apoptosis of T cells, probably through the induction of death effector genes such as p53 (Dumont et al., 1999). Thus, although NF-κB plays a pivotal antiapoptotic role in serum-deprived apoptosis of NIH3T3, the role of NF-κB in the regulation of cell survival is supposed to be essentially different according to the induced target molecule (e.g., MnSOD, Bcl-XL, Fas-ligand, or p53) that plays the most decisive role in host cells.

Experimental Procedures

Reagents and Antibodies

The antibodies (Abs) against E2F1 (C-20, KH95), p65 NF-κB (C-20), p50 NF-κB (C-19), caspase-3 (H-277), c-Myc (C-33), HA (Y-11), Actin (C-11), and PCNA (PC10) were purchased from Santa Cruz Biotechnology (Santa Cruz, CA); an anti-cytochrome c Ab from Pharmingen (Pharmingen, CA); and an anti-Flag Ab (M2) from Sigma (St Louis, MO).

Cells and Cultures

NIH3T3, Saos-2, and 293T were maintained in DMEM containing 10% fetal bovine serum (FBS). Wild-type and E2F$^{-/-}$ MEFs were kindly provided from Drs. L. Jakoi and J.R. Nevins (Duke University Medical Center, NC) and were cultured in DMEM containing 15% FBS.

Plasmid Constructs and cDNAs

Expression vectors for wt E2F1-4 and mutant E2F1s (1-88, 113-120, E132, 206-220, and 411/421) were provided from Dr. J. R. Nevins (Cress et al., 1993). The other mutant E2F1s were constructed by the PCR method. Other expression vectors or cDNAs were gifts of the investigators as follows: MnSOD from K. Scharffetter-Kochanek

(University of Cologne, Hamburg, Germany), Cu/ZnSOD from M.V. Clement (National University of Singapore, Singapore), DP-1 from Dr. N. Dyson (Massachusetts General Hospital Cancer Center, Charlestown, MA), p65 and p50 NF-κB from Dr. S. Hai (Ohio State University, OH), and dn NF-κB from Dr. D.W. Ballard (Vanderbilt University School of Medicine, TN).

Coimmunoprecipitation Analysis and Immunoblotting

Coimmunoprecipitation analysis and immunoblotting were performed as described previously (Matsumura et al., 2000).

Preparation of Stable Transfectants

We transfected an expression vector for c-Myc, E2F1, or c-MycERT together with pSV2neo into NIH3T3 and Saos-2 and selected the clones by the culture with 1.0 mg/ml of G418. To further transfect an expression vector of MnSOD into G418-resistant clones, we cotransfected pBabe-puro and selected the clones by the culture with 1.0 μg/ml of puromycin.

Northern Blot Analysis

The method for Northern blot was described previously (Matsumura et al., 1999).

DNA Content Analysis

DNA content of the cells was quantitated by staining with propidium iodide (PI) and analyzed on FACSort (Beckon Dickinson, Oxnard, CA).

Detection of $\Delta\Psi m$

We examined $\Delta\Psi m$ with DePsioher (Trevigen, Gaitherburg, MD) by flow cytometry or fluorescence microscopy according to the manufacturer's instructions.

Detection of ROS

To detect ROS by flow cytometry or fluorescence microscopy, we used RedoxSensor Red CC-1 (R14060), dihydroethidium (D-1168) or CM-H2DCFDA (C-6827) (Molecular Probes, Eugene, OR).

Fluoreacence Microscopy

The cells were stained with Mitotracker Green FM stain (M-7514) (Molecular Probes) and RedoxSensor Red CC-1 to detect ROS accumulation, with DePsioher to evaluate $\Delta\Psi m$, or with Hoechist 33342 (H-3570) (Molecular Probes) to visualize nucleus. The cells were analyzed with a Zeiss Axioplan microscope (Zeiss LSM410, Obercochen, Germany) and a Bio-Rad Lasershape MRC 500 scanning confocal microscopy system (Bio-Lad Laboratories, Richmond, CA).

Detection of Apoptotic Cells by Fluoreecent Microscopy

To distinguish the cells transfected with the effector gene, we cotransfected an expression vector of Discosoma sp red fluorescent protein (pDsRed2-N1) (CLONTECH, Palo Alto, CA) and detected apoptotic cells with Annexin-V-EGFP (K2019-2) (CLONTECH) by fluorescent microscopy.

Fractionation of Mitochondria and Cytosol and Measurement of MnSOD Activity

We isolated mitochondrial protein from cytosolic protein with an ApoAlert Cell Fractionation Kit (CLONTECH). Mitochondrial MnSOD activity was measured by a Mn-SOD ELISA System RPJ301 (Amersham, Uppsala, Sweden).

Construction of MnSOD Reporter Genes

−2505-SOD-Luc in which 2525 bp of rat MnSOD promoter (−2505 to +20) was subcloned into pGL3-basic-Luc (Promega, Madison, WI) was provided from Dr. M.I. Darville (Vrije Univeiteit Brussel, Brussels, Belgium) (Darvile et al., 2000). A series of deletion mutants of MnSOD promoter were generated by the PCR method. The core sequences of wt and mutated NF-κB binding sites are as follows: SOD-κB-1 (GGGTCTTCCC), SOD-κB-1m (CCCTCTTCCC), SOD-κB-2 (GGGGCTTTCC), SOD-κB-2m (CCCGCTTTCC), and IgκE (GGGAATTTCC).

Luciferase Assays

Luciferase assays were performed with a Dual-Luciferase Reporter System (Promega) as previously described (Matsumura et al., 1999). To examine the effects of AS-E2F1, S-E2F1, and MM-CTL oligonucleotides, we transfected 12 μg of each FITC-labeled phosphorothioated oligonucleotide into NIH3T3 cells together with 0.5 μg of 3×IgκE-Luc and 10 ng of pRL-CMV-luc by TransFast transfection reagent (Promega). After 24 hr, the cells with strong FITC intensity were sorted by FACS vantage (Beckton Dickinson) and subjected to further analyses. The sequences of oligonucleotides are as follows: AS-E2F1, 5′-CCGGCCAAGGCCATGAC-3′ (−3 to +14); S-E2F1, 5′-GTCATGGCCTTGGCCGG-3′; and MM-CTL, 5′-ACTGCGATG GACGTGTC-3′.

EMSA

EMSA was performed as previously described (Matsumura et al., 1999). Three types of double-stranded oligonucleotides (IgκE, SOD-κB-1, and SOD-κB-2) were used as a probe or a competitor, and their sequences are described above.

GST Pull-Down Experiments

^{35}S-labeled E2F1 was prepared by a TNT reticulocyte lysate system (Promega). pGEX-3X-3, pGEX-3X-3-p65 (1-305), and pGEX-3X-3-p65 (354-551) were provided by Dr. H. Sakurai (Tanabe Seiyaku C. Ltd., Osaka, Japan). pGEX-3X-3-p65 (168-291) was constructed by the PCR method. Purification of GST-p65 fusion proteins and the in vitro binding reaction were performed as previously described (Sakurai et al., 1999).

Acknowledgments

We especially thank Drs. J.R. Nevins and L. Jakoi for providing wt and E2F1$^{-/-}$ MEFs and several expression vectors. We thank Drs. K. Scharffetter-Kochanek, M.V. Clement, N. Dyson, S. Hai, D.W. Ballard, M.I. Darville, and H. Sakurai for providing the plasmids.

Received: August 31, 2001
Revised: March 11, 2002

References

Adler, V., Yin, Z., Tew, K.D., and Ronai, Z. (1999). Role of redox potential and reactive oxygen species in stress signaling. Oncogene *18*, 6104–6111.

Barkett, M., and Gilmore, T.D. (1999). Control of apoptosis by Rel/NF-kB transcription factors. Oncogene *18*, 6910–6924.

Bates, S., Phillips, A.C., Clark, P.A., Stott, F., Peters, G., Ludwig, R.L., and Vousden, K.H. (1998). p14ARF links the tumour suppressors RB and p53. Nature *395*, 124–125.

Beg, A.A., Sha, W.C., Bronson, R.T., Ghosh, S., and Baltimore, D. (1995). Embryonic lethality and liver degeneration in mice lacking the RelA component of NF-kB. Nature *376*, 167–170.

Benhar, M., Dalyot, I., Engelberg, D., and Levitzki, A. (2001). Enhanced ROS production in oncogenically transformed cells potentiates c-Jun N-terminal kinase and p38 mitogen-activated protein kinase activation and sensitization to genotoxic stress. Mol. Cell. Biol. *21*, 6913–6926.

Cai, J., Yang, J., and Jones, D.P. (1998). Mitochondrial control of apoptosis: the role of cytochrome c. Biochim. Biophys. Acta *1366*, 139–149.

Cress, W.D., Johnson, D.G., and Nevins, J.R. (1993). A genetic analysis of the E2F1 gene distinguishes regulation by Rb, p107, and adenovirus E4. Mol. Cell. Biol. *13*, 6314–6325.

Dang, C.V. (1999). c-Myc target genes involved in cell growth, apoptosis, and metabolism. Mol. Cell. Biol. *19*, 1–11.

Darville, M.I., Ho, Y.S., Eizirik, D.L. (2000). NF-kB is required for cytokine-induced manganese superoxide dismutase expression in insulin-producing cells. Endocrinology *141*, 153–162.

Dumont, A., Hehner, S.P., Hofmann, T.G., Ueffing, M., Droge, W., and Schmitz, M.L. (1999). Hydrogen peroxide-induced apoptosis is CD95-independent, requires the release of mitochondria-derived

reactive oxygen species and the activation of NF-kB. Oncogene *18*, 747–757.

Field, S.J., Tsai, F.Y., Kuo, F., Zubiaga, A.M., Kaelin, W.G., Jr., Livingston, D.M., Orkin, S.H., and Greenberg, M.E. (1996). E2F-1 functions in mice to promote apoptosis and suppress proliferation. Cell *85*, 549–561.

Goldman, R., Moshonov, S., and Zor., U. (1998). Generation of reactive oxygen species in a human keratinocyte cell line: role of calcium. Arch. Biochem. Biophys. *350*, 10–18.

Greenlund, L.J., Deckwerth, T.L., and Johnson, E.M., Jr. (1995). Superoxide dismutase delays neuronal apoptosis: a role for reactive oxygen species in programmed neuronal death. Neuron *14*, 303–315.

Harbour, J.W., and Dean, D.C. (2000). The Rb/E2F pathway: expanding roles and emerging paradigms. Genes Dev. *14*, 2393–2409.

Hsieh, J.K., Fredersdorf, S., Kouzarides, T., Martin, K., and Lu, X. (1997). E2F1-induced apoptosis requires DNA binding but not transactivation and is inhibited by the retinoblastoma protein through direct interaction. Genes Dev. *11*, 1840–1852.

Huang, C., Zhang, Z., Ding, M., Li, J., Ye, J., Leonard, S.S., Shen, H.M., Butterworth, L., Lu, Y., Costa, M., et al. (2000). Vanadate induces p53 transactivation through hydrogen peroxide and causes apoptosis. J. Biol. Chem. *275*, 32516–32522.

Irwin, M., Marin, M.C., Phillips, A.C., Seelan, R.S., Smith, D.I., Liu, W., Flores, E.R., Tsai, K.Y., Jacks, T., Vousden, K.H., et al. (2000). Role for the p53 homologue p73 in E2F-1-induced apoptosis. Nature *407*, 645–648.

Jones, P.L., Ping, D., and Boss, J.M. (1997). Tumor necrosis factor alpha and interleukin-1b regulate the murine manganese superoxide dismutase gene through a complex intronic enhancer involving C/EBP-b and NF-kB. Mol. Cell. Biol. *17*, 6970–6981.

Leone, G., Sears, R., Huang, E., Rempel, R., Nuckolls, F., Park, C.H., Giangrande, P., Wu, L., Saavedra, H.I., Field, S.J., et al. (2001). Myc requires distinct E2F activities to induce S phase and apoptosis. Mol. Cell *8*, 105–113.

Lissy, N.A., Davis, P.K., Irwin, M., Kaelin, W.G., and Dowdy, S.F. (2000). A common E2F-1 and p73 pathway mediates cell death induced by TCR activation. Nature *407*, 642–645.

Matsumura, I., Kitamura, T., Wakao, H., Tanaka, H., Hashimoto, K., Albanese, C., Downward, J., Pestell, R.G., and Kanakura, Y. (1999). Transcriptional regulation of the cyclin D1 promoter by STAT5: its involvement in cytokine-dependent growth of hematopoietic cells. EMBO J. *18*, 1367–1377.

Matsumura, I., Kawasaki, A., Tanaka, H., Sonoyama, J., Ezoe, S., Minegishi, N., Nakajima, K., Yamamoto, M., and Kanakura, Y. (2000). Biologic significance of GATA-1 activities in Ras-mediated megakaryocytic differentiation of hematopoietic cell lines. Blood *96*, 2440–2450.

Moroni, M.C., Hickman, E.S., Denchi, E.L., Caprara, G., Colli, E., Cecconi, F., Muller, H., and Helin, K. (2001). Apaf-1 is a transcriptional target for E2F and p53. Nat. Cell Biol. *3*, 552–558.

Muller, H., Bracken, A.P., Vernell, R., Moroni, M.C., Christians, F., Grassilli, E., Prosperini, E., Vigo, E., Oliner, J.D., and Helin, K. (2001). E2Fs regulate the expression of genes involved in differentiation, development, proliferation, and apoptosis. Genes Dev. *15*, 267–285.

Nip, J., Strom, D.K., Eischen, C.M., Cleveland, J.L., Zambetti, G.P., and Hiebert, S.W. (2001). E2F-1 induces the stabilization of p53 but blocks p53-mediated transactivation. Oncogene *20*, 910–920.

Phillips, A.C., Bates, S., Ryan, K.M., Helin, K., and Vousden, K.H. (1997). Induction of DNA synthesis and apoptosis are separable functions of E2F-1. Genes Dev. *11*, 1853–1863.

Phillips, A.C., Ernst, M.K., Bates, S., Rice, N.R., and Vousden, K.H. (1999). E2F-1 potentiates cell death by blocking antiapoptotic signaling pathways. Mol. Cell *4*, 771–781.

Polyak, K., Xia, Y., Zweier, J.L., Kinzler, K.W., and Vogelstein, B. (1997). A model for p53-induced apoptosis. Nature *389*, 300–305.

Rhee, S.G. (1999). Redox signaling: hydrogen peroxide as intracellular messenger. Exp. Mol. Med. *31*, 53–59.

Ryan, K.M., Ernst, M.K., Rice, N.R., and Vousden, K.H. (2000). Role of NF-kB in p53-mediated programmed cell death. Nature *404*, 892–897.

Sakurai, H., Chiba, H., Miyoshi, H., Sugita, T., and Toriumi, W. (1999). IkB kinases phosphorylate NF-kB p65 subunit on serine 536 in the transactivation domain. J. Biol. Chem. *274*, 30353–30356.

Sawada, M., Nakashima, S., Kiyono, T., Nakagawa, M., Yamada, J., Yamakawa, H., Banno, Y., Shinoda, J., Nishimura, Y., Nozawa, Y., et al. (2001). p53 regulates ceramide formation by neutral sphingomyelinase through reactive oxygen species in human glioma cells. Oncogene *20*, 1368–1378.

Sherr, C.J., and Roberts, J.M. (1999). CDK inhibitors: positive and negative regulators of G1-phase progression. Genes Dev. *13*, 1501–1512.

Sorensen, T.S., Girling, R., Lee, C.W., Gannon, J., Bandara, L.R., and La Thangue N.B. (1996). Functional interaction between DP-1 and p53. Mol. Cell. Biol.*16*, 5888–5895.

Suzuki, Y., Ono, Y., and Hirabayashi, Y. (1998). Rapid and specific reactive oxygen species generation via NADPH oxidase activation during Fas-mediated apoptosis. FEBS Lett. *425*, 209–212.

Yamasaki, L., Jacks, T., Bronson, R., Goillot, E., Harlow, E., and Dyson, N.J. (1996). Tumor induction and tissue atrophy in mice lacking E2F-1. Cell *85*, 537–548.

Zindy, F., Eischen, C.M., Randle, D.H., Kamijo, T., Cleveland, J.L., Sherr, C.J., and Roussel, M.F. (1998). Myc signaling via the ARF tumor suppressor regulates p53-dependent apoptosis and immortalization. Genes Dev. *12*, 2424–2433.

Journal of Biological Sciences 5 (1): 50-60, 2005
ISSN 1727-3048

Cell Cycle Regulation in Hematopoietic Stem/progenitor Cells

[1,2]Hirokazu Tanaka, [2]Itaru Matsumura and [2]Yuzuru Kanakura
[1]Regenerative Medicine, Foundation for Biomedical Research and Innovation, Kobe, Japan
[2]Department of Hematology and Oncology,
Osaka University Graduate School of Medicine, Suita, Osaka, Japan

Abstract: Hematopoietic Stem Cells (HSCs) are characterized by two distinct abilities, that is, self-renewal ability and multipotency. To keep the homeostasis of hematopoiesis and protect the exhaustion of HSCs throughout the life, most of HSCs are kept quiescent and only a limited number of HSCs enter cell cycle to supply mature blood cells. Cell cycle state of HSCs is crucially regulated by external factors such as cytokines, Notch ligands and Wnt signals in the Bone Marrow (BM) microenvironment, so called hematopoietic niche. In addition, the intrinsic factors expressed in HSCs such as c-Myb, GATA-2, HOX family proteins and Bmi-1 also control their growth through the gene transcription. Cell cycle regulation in HSCs is not so unique but rather common to other cell types. However, the specific function of each cell cycle regulatory molecule in HSCs has been clarified during the last few years. Especially, $p21^{WAF1}$ and $p18^{INK4C}$ keep the quiescence of HSCs and $p27^{CIP1}$ keeps that of progenitor cells, respectively, thereby governing their pool sizes and/or preventing their exhaustion. On the other hand, the inactivation or deletion of $p16^{INK4A}$ and $p15^{INK4B}$ genes is supposed to contribute to malignant transformation of hematopoietic cells. These results imply that appropriate cell cycle control at the stage of stem/progenitor cells in the BM is required for maintaining normal hematopoiesis.

Key words: Hematopoietic stem/progenitor cell, cell cycle

INTRODUCTION

HSCs are characterized by two distinct abilities; self-renewal ability and multipotency. With these activities, HSCs are capable of maintaining a life-long supply of all lineages of hematopoietic cells according to systemic needs. The durability of the output potential of HSCs is believed to be dependent on their ability to execute self-renewal divisions; that is, an ability to proliferate without activation of a latent readiness to differentiate along restricted lineages. To maintain the homeostasis of hematopoiesis and protect the exhaustion of HSC population, most of HSCs are kept quiescent and only a limited number of cells enter cell cycle to supply mature blood cells. During this cell division, HSCs are obliged to undergo self-renewal, differentiation, or apoptosis. This step is controlled by external stimuli transmitted from the Bone Marrow (BM) microenvironment, including cytokines, Notch ligands, Wnt signals and sonic hedgehog (Shh) signals. Also, intrinsic factors expressed in HSCs, such as transcription regulators and cell cycle regulatory molecules, are crucially involved in this regulation (Fig. 1).

During the last decade, a number of cell cycle regulatory molecules such as cyclins, Cyclin-dependent Kinases (CDKs) and CDK inhibitors (CKIs) have been identified and their roles and regulation have been well characterized in various types of cells[1-3]. Cell cycle is positively regulated by CDKs associated with cyclins and their activities are negatively regulated by CKIs also included in these complexes at the same time. CKIs are classified into two families based on their structures and CDK targets. One class of inhibitors including $p21^{WAF1}$ (hereafter indicated as p21), $p27^{KIP1}$ (p27) and$p57^{KIP2}$ share a CDK2-binding motif in the N-terminus and inhibit the activities of cyclinD-, E- andA-dependent kinases. The other class of inhibitors also known as the INK4 family, including $p16^{INK4A}$ (p16), $p15^{INK4B}$ (p15), $p18^{INK4C}$ (p18) and $p19^{INK4D}$, contain fourfold ankyrin repeats and specifically inhibit CDK4 and CDK6. Members of both families are important for executing cell cycle arrest in response to a variety of stimuli such as DNA damage, contact inhibition and transforming growth factor-β1 (TGF-β1) treatment.

Molecular mechanisms governing the stemness of HSCs from a viewpoint of cell cycle regulation are presented in this study.

Corresponding Author: Itaru Matsumura, M.D., Ph.D., Department of Hematology and Oncology,
Osaka University Graduate School of Medicine, 2-2, Yamada-oka, Suita, Osaka 565-0871, Japan
Tel: +81-6-6879-3871 Fax: +81-6879-3879 E-mail: matumura@bldon.med.osaka-u.ac.jp

Characteristic of HSCs: The procedure for the purification of HSCs has made great progress along with the identification of molecular markers that characterize the cells having reconstitution activities in transplanted mice. The most primitive HSCs are considered to be with the $CD34^{low/-}c\text{-}Kit^{+}Sca\text{-}1^{+}Lin^{-}$ (CD34-KSL) phenotype, since a single cell with this phenotype could reconstitute whole hematopoiesis *in vivo* with high probability[4]. In addition to the specific surface phenotype, HSCs present in steady-state adult mouse BM are functionally characterized by their ability to efflux Rhodamine-123 and Hoechst 33342[5,6]. When adult mouse BM cells are stained with Hoechst 33342, exposed to the UV light and examined at 2 emission wavelengths simultaneously, HSCs are found in the rare Side Population (SP) with the dim fluorescence because of this ability[7]. The low fluorescence of HSCs after staining with Rhodamine-123 and Hoechst 33342 is attributed to their selective expression of different ABC transporters, P-glycoprotein and berp-1, respectively[8-10]. In addition, a more recent study proved that the cells having the strongest dye efflux capacity (Tip-SP cells) with the CD34-KSL phenotype are the most primitive HSCs, which can reconstitute long-term hematopoiesis with almost 100% probability after the single cell transplantation[11]. The cells in the SP fraction is considered to be in the G0 phase and this state is supposed to be restrictedly regulated by "hematopoietic niche" in the BM as described later.

Cytokines involved in cell cycle regulation in HSCs: A number of cytokines regulate growth, differentiation and survival of HSCs both positively and negatively. Among these, stem cell factor (SCF), Flt3 ligand (FL), thrombopoietin (TPO), interleukin-3 (IL-3) and IL-6 are known to promote the growth of HSCs *in vitro*[12-14]. In fact, Sl/Sl and W/W mice each having homozygous defect in the SCF gene and its receptor c-kit gene reveal severe anemia[15]. Also, total number of HSCs was reduced in the BM of c-mpl (TPO receptor)-null mice[16]. In addition, HSCs obtained from $c\text{-}mpl^{-/-}$ mice reveled severely decreased activities in reconstitution assays. These lines of evidence indicate that cytokine signals are required for the growth and survival of HSCs *in vivo* as well as *in vitro*[17].

During the last few years, the number of cases with hematologic malignancies receiving cord blood transplantation has increased more and more. However, the insufficient number of HSCs in each cord blood and the delayed recovery of hematopoiesis have limited their applicability to transplantation for adults. So, it has been of particular interest to expand hematopoietic cells *ex vivo*. Regarding the effects of cytokines in the *ex vivo* expansion of HSCs, a number of cytokine combinations were employed and their effects were evaluated by long-term reconstitution assays in transplanted mice. Among these, the combination of SCF, FL, TPO and IL-6/soluble IL-6 receptor seems to induce the *ex vivo* expansion of HSCs most efficiently with 4.2-fold increase of SRC (SCID-repopulating cells)[18].

TGF-β1 is a 25 kd protein produced by the stromal cells and by the hematopoietic progenitors, which induces the growth arrest in HSCs in autocrine and/or paracrine manners[19-23]. Using antisense oligonucleotides, it was demonstrated that the inhibition of TGF-β1 production could release HSCs in the umbilical cord blood or BM from quiescence[22,24,25]. Furthermore, the inhibition of the TGF-β1 signaling pathways in human HSCs using blocking antibodies against TGF-β1 or its receptor allowed quiescent cells to enter the cell cycle[26]. TGF-β1 has been supposed to induce cell-cycle arrest through p21 and p27 in various cell types including HSCs[27-33]. However, a recent paper provided evidence that TGF-β1 induces growth arrest independently of p21 or p27 by demonstrating that TGF-β1 can suppress the growth of HSCs and progenitor cells lacking both p21 and p27[34]. As for the other possible mechanisms of TGF-β1-induced growth arrest, TGF-β1 was reported to transcriptionally induce the expression of p15[35,36] and to down regulate the expression of c-Kit, FLT3 andIL-6 receptor on HSCs, thereby disrupting cytokine-dependent growth signals[37,38].

In contrast, another TGF-β super family protein, bone morphogenetic protein-4 (BMP-4) was recently reported to induce self-renewal of HSCs[39].

Effects of the BM microenvironment "hematopoietic niche" on cell cycle regulation in HSCs: HSCs receive critical signals for proliferation and differentiation from the BM microenvironment consisting of stromal cells and the extracellular matrix (ECM)[40-42]. ECM is composed of a variety of molecules such as fibronectin (FN), collagens, laminin and proteoglycans. ECM in the BM is not merely an inert framework but mediates specialized functions[43-45]. Some components of ECM have been shown to bind to growth factors produced by stromal cells and to immobilize them around cells, resulting in giving spaces where hematopoietic cells and growth factors colocalize. In addition, ECM can bind to glycoproteins expressed on HSCs. FN, collagens and laminin are ligands for integrins that not only control anchorage, spreading and migration of HSCs but also activate signal transduction pathways in these cells[43,44,46,47].

As were the cases with the niches for gut and certain skin stem cells[48-52], it has been supposed that HSCs also receive critical signals for proliferation and differentiation from the BM microenvironment "hematopoietic niche". However, it has been unknown where the hematopoietic niche is located in the BM or what types of cells

contribute to it. Recently, two groups individually generated mice lacking the BMP receptor type A (BMPRIA) and those engineered to produce osteoblast-specific, activated Parathyroid Hormone (PTH) and PTH-related protein (PTHrP) receptors (PPRs). In these mice, the osteoblast population was found to increase in the specific regions of bone, 'trabecular bone-like areas'. Also, the increase of the osteoblast population caused the parallel increase of the HSC population, particularly long-term repopulating HSCs[51,52]. As for this mechanism, Zhang *et al.*[51] demonstrated that the long-term HSCs were attached to spindle-shaped N-cadherin$^+$CD45$^-$ osteoblastic (SNO) cells. Two adherent junction molecules, N-cadherin and β-catenin, were asymmetrically localized between the SNO cells and the long-term HSCs, suggesting that SNO cells function as a key component of the niche to support HSCs and that BMP signaling through BMPRIA controls the number of HSCs by regulating niche size. Meanwhile, in the latter study, Calvi *et al.*[52] demonstrated that PPR-stimulated osteoblasts produced high levels of the Notch1 ligand, Jagged1 and supported the activity of HSCs through the Notch signaling. Together, these papers indicate that the interaction with osteoblasts contributes to the maintenance of the HSCs.

HSCs expressing the receptor tyrosine kinase Ties were quiescent and Ang-1, the ligand for Tie2 expressed on endothelial cells and HSCs, enhanced the quiescence of HSCs and their adhesion to fibronectin and collagen[53,54]. Therefore, it has been assumed that the Ang-1/Tie2 signaling pathway plays some role in the quiescence of HSCs. In accord with this hypothesis, a recent paper proved that Tie2$^+$ HSCs were in close contact with sub-endosteal osteoblasts expressing Ang-1 and that these Tie2$^+$ cells were included in SP and in the G0 phase of the cell cycle in the pyronin Y staining[55]. These results suggest that HSCs attaching to the specific osteoblasts in the hematopoietic niche are kept quiescent and protected from the myelosuppressive stress such as the treatment with 5-Fluorouracil (5-FU), a cell cycle-specific myelotoxic agent that kills cycling cells. However, it remains unknown which fraction of osteoblasts expresses Ang-1 and how it is regulated. Furthermore, the molecular mechanisms how Tie2/Ang-1 signaling prevents cell cycle progression also remain elusive.

Effects of the signals from the Notch ligand, Wnt and sonic hedgehog (Shh) on self-renewal of HSCs: In addition to the cytokines and molecules consisting of the extracellular matrix, various stimuli such as the Notch ligand, Wnt and Shh are transmitted to HSCs in the BM microenvironment. The activation of Notch transmembrane receptors expressed on HSCs by their ligand (Jagged 1 or Jagged 2) expressed on stromal cells promotes self-renewal of HSCs[56-60]. As for the critical target molecule of Notch signals that mediates self-renewal of HSCs, we recently found that c-Myc was transcriptionally induced by Notch[61]. In addition, the ectopic expression of c-Myc induced the growth of HSCs without disrupting their biologic properties in terms of surface phenotypes, colony-forming activities and reconstituting activities. Thus, c-Myc was supposed to play a major role in self-renewal of HSCs as an effector molecule of Notch signals.

Like Jagged1/Notch, a number of Wnt proteins are expressed in the BM and their receptor frizzled was detectable on BM-derived HSCs and progenitor cells[62,63]. Reya *et al.*[64] recently demonstrated that the Wnt signaling is important for the *in vitro* and *in vivo* self-renewal of normal HSCs. Moreover, they demonstrated that the activation of Wnt signaling in HSCs induces the increased expression of HOXB4 and Notch1, thereby inducing proliferation of HSCs. Besides Wnt3a that activates the canonical pathway through Frizzled/β-catenin/TCF/LEF, non-canonical Wnt, Wnt-5a, was also reported to expanded HSCs *in vitro*[65]. However, its mechanisms remain to be clarified.

Shh is a family member of human homologs of *Drosophila* Hedgehog (Hh) and expressed on the cell surface as transmembrane proteins. Hh signals can be mediated through cell-to-cell contact between adjacent cells expressing the Patched (Ptc) receptor. Alternatively, NH2-terminal cleavage of Hh can generate a soluble Hh ligand that can interact with distal cells expressing Ptc[66,67]. In the BM, Shh and their receptors Ptc and Smoothened (Smo) are expressed in highly purified HSCs. Cytokine-induced proliferation of HSCs could be inhibited by the anti-Hh Ab, implying that endogenously produced Hh proteins play a role in the expansion of HSCs. Addition of soluble forms of Shh resulted in an increase in the number of HSCs with pluripotent repopulating capacities. In addition, Noggin, a potent BMP-4 inhibitor, was found to inhibit the mitogenic effects of Shh, indicating that Shh signaling acts upstream of BMP-4 signaling to induce proliferation of HSCs[68].

Intrinsic factors that regulate the growth of HSCs: In addition to extrinsic factors, accumulated evidence indicates that cell cycle state of HSCs is regulated by intrinsic transcription regulatory factors, such c-Myb, GATA-2, HOX proteins and Bmi-1 (Fig. 2).

A transcriptional factor, c-Myb promotes the growth of HSCs, probably through the induction of c-myc and upregulated expression of c-kit and Flt3[69,70] and c-Myb-deficient mice die at embryonic day 15.5 (E15.5) due to the defect of definitive hematopoiesis[71]. Similarly, GATA-2$^{-/-}$

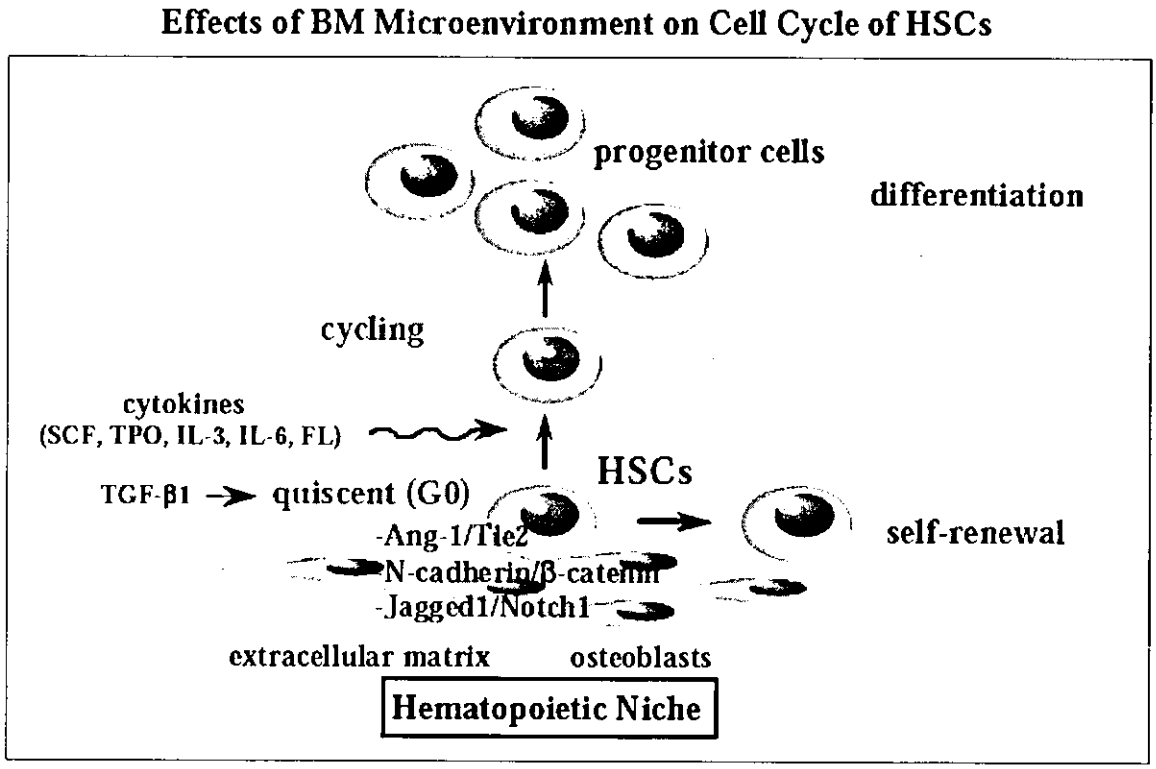

Fig. 1: Effects of BM microenvironment on cell cycle of HSCs

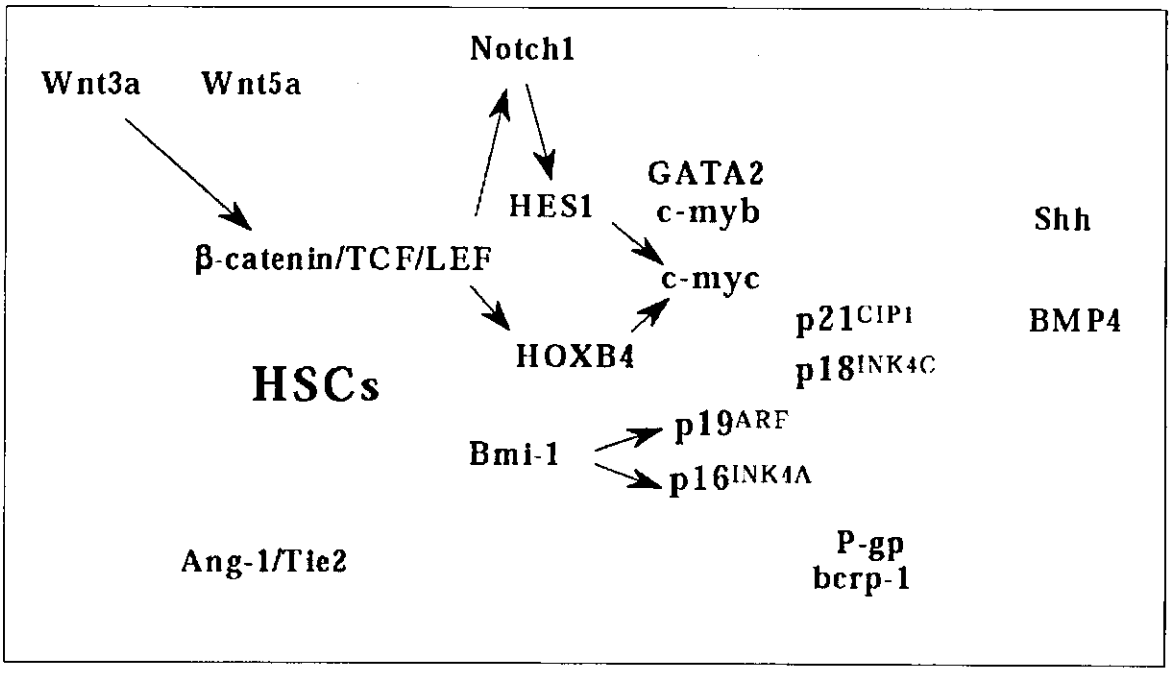

Fig. 2: Regulation of stemness by intrinsic factors in HSCs

mice are embryonic lethal around E11.5 because of the defect in the development and/or maintenance of HSCs[72]. However, functional roles of GATA-2 in the growth of HSCs are still controversial[73-76]. So, it remains unknown whether GATA-2 enhances or suppresses the growth of HSCs.

Among HOX family of transcription factors, HOXB4 is of particular remark as it promotes the growth of HSCs without the induction of leukemias[77-79]. As a result of the HOXB4 gene transfer or the protein delivery, HSCs could be expanded retaining their normal *in vivo* potential of differentiation and long-term repopulation[78,80]. Moreover, a recent study using HOXB4$^{-/-}$HOXB3$^{-/-}$ mice demonstrated that both HOXB4 and HOXB3 are required for the maximal growth potential of HSCs[81].

Bmi-1, a member of the Polycomb Group family of transcriptional repressors[82], was recently shown to be essential for maintenance of adult self-renewing HSCs[83]. Although the number of HSCs in the fetal liver of Bmi-1$^{-/-}$ mice was normal, the number of HSCs was markedly reduced in postnatal Bmi-1$^{-/-}$ mice. Furthermore, transplanted fetal liver and bone marrow cells obtained from Bmi-1$^{-/-}$ mice were able to contribute to hematopoiesis only transiently. Regarding this mechanism, in accord with the previous data obtained from embryonic fibroblasts[84], the micro array analysis on the BM mononuclear cells isolated from wild-type and Bmi-1$^{-/-}$ mice showed that the expression of p16 and p19^{ARF}, which is generated from the same INK4A locus by alternative splicing and inhibits MDM-2-mediated p53 degradation, was upregulated in Bmi-1$^{-/-}$ BM cells.

During neural development in mouse embryos, the cell-cycle regulator geminin controls replication by binding to the licensing factor Cdt1[85,86]. Recently, Luo *et al.*[87] reported that murine geminin transiently associated with members of the HOX-repressing polycomb complex, with the chromatin of HOX regulatory DNA elements and with HOX proteins[87]. Through these interactions, geminin displaces HOX proteins from their target genes and/or can interact with polycomb proteins to influence HOX activities. Therefore, the activities of HOX and polycomb protein families might be similarly regulated in HSCs.

Roles of p21 and p27 in quiescence of HSCs and progenitor cells: Embryonic fibroblasts obtained from p21$^{-/-}$ mice had a defect in their ability to achieve cell cycle arrest after irradiation[88,89] and antisense oligonucleotides against p21 was shown to release human mesenchymal cells from G0[90]. Therefore, p21 is required for the cell cycle arrest in G0 or G1 in some cell types. As for the roles for p21 in hematopoiesis, the expression level of p21 was reported be low in CD34$^+$ cells[91,92] and p21$^{-/-}$ mice did not exhibit an apparent hematologic defect[88,89]. However, in a subsequent analysis, Cheng *et al.*[93] found that p21 was highly expressed in the quiescent stem cell-like fraction of BM cells[93]. They also found that, under normal homeostatic conditions, the proportion of quiescent HSCs in the G0 phase was reduced and that total number of HSCs increased in p21$^{-/-}$ mice. In accord with these findings, when p21$^{-/-}$ mice were treated with 5-FU, the survival percentage was much lower in p21$^{-/-}$ mice than in littermate controls. They also directly assessed stem cell self-renewal capability using a serial transplantation approach. As a result, no mice transplanted with p21$^{-/-}$ BM cells survived after the fifth transplant due to the exhaustion of HSC population, whereas those transplanted with p21$^{+/+}$ BM cells had a 50% survival. Together, these results indicate that p21 is a key molecule that restricts cell cycle entry of HSCs, thereby keeping their pool size and preventing their exhaustion under certain stress.

p27 is molecularly distinct from p21 in its carboxyl terminus; it interacts with similar, though not identical, cyclin-CDK complex and lacks p53-regulated expression. In hematopoietic system, the expression of p27 is observed in more mature progenitors than p21[91,92]. The p27$^{-/-}$ mice have a larger body and hyperplasia of most organs including hematopoietic organs[94-96]. In striking contrast to p21$^{-/-}$ mice, the number, cell cycling and self-renewal of HSCs were normal in p27$^{-/-}$ mice, while these mice had an increase in hematopoietic progenitor cells[97]. In addition, these progenitor cells in p27$^{-/-}$ mice were more proliferative than p27$^{+/+}$ progenitor cells. Furthermore, progenitor cells from p27$^{-/-}$ mice were able to expand and regenerate hematopoiesis after serial transplantation, while p27$^{+/+}$ progenitors were markedly depleted. Thus, p21 and p27 govern the divergent stem and progenitor cell populations, respectively.

Roles for the INK4 family in self-renewing division of HSCs and as tumor suppressor genes: Several of INK4 proteins have been supposed to be implicated in the regulation of HSCs numbers and self-renewal. Yuen *et al.*[98] recently clarified a function of p18 in HSCs and the early progenitor cells[98]. Mice deficient for p18 had an increased number of HSCs in the bone marrow. Also, competitive repopulation assays showed that p18$^{-/-}$ HSCs are far more competitive than normal HSCs with 14-fold activities. In contrast to p21$^{-/-}$ HSCs, the exhaustion of p18$^{-/-}$ HSCs was not observed during serial bone marrow transplants, indicating that p18 is a strong inhibitor limiting the potential of stem cell self-renewal *in vivo*.

On the other hands, p16 is highly expressed in CD34$^+$ cells and its expression is down regulated during differentiation process towards all lineages[99]. So, p16 was assumed to play some role in cell cycle arrest in HSCs. However, since p16$^{-/-}$ mice did not show an apparent

abnormality in hematopoiesis, p16 was supposed to be dispensable for the quiescence of HSCs[100,101]. In contrast to the expression pattern of p16, the expression of p15 was not detected in $CD34^+$ cells, but increased specifically during myeloid differentiation[99,102]. However, the functional role of p15 in HSCs remained to be clarified. Both p16 and p15 inhibit the function of cyclin D-CDK4/6 complex and suppress the phosphorylation of pRb, thereby inducing cell cycle arrest at G0/G1 phase. Especially, under tumorgenetic stress such as the presence of oncogenic ras gene, p16 and p15 are induced to express and suppress tumor progression through the induction of premature senescence[103,104]. With these activities, both p16 and p15 are supposed to act as tumor suppressor genes. In fact, inactivation and/or deletion of p16 and p15 genes are observed in various human cancers very frequently[105,106]. As for hematologic malignancies, their defects caused by the homozygotic deletion or methylation were observed in a substantial proportion of AML, ALL, ATL, malignant lymphoma and MDS cases[107-111]. These results indicate that appropriate cell cycle control, particularly at the stage of stem/progenitor cells, is required for maintaining normal hematopoiesis.

CONCLUSIONS

Although a great advance has been made in stem cell biology, particularly in terms of purifying and evaluating the function of HSCs, precise mechanisms of cell cycle regulation that assign self-renewal or differentiation to HSCs remain unknown. So, further studies are required to disclose the whole feature of cell cycle regulation in HSCs. These studies would undoubtfully bring about useful information to establish therapeutic strategies for *ex vivo* stem cell expansion.

REFERENCES

1. Roberts, J.M., 1999. Evolving ideas about cyclins. Cell, 98: 129-132.
2. Morgan, D.O., 1995. Principles of CDK regulation Nature, 374: 131-134.
3. Sherr, C.J. and J.M. Roberts, 1999. CDK inhibitors: positive and negative regulators of G1-phase progression. Gen. Dev., 13: 1501-1512.
4. Osawa, M., K. Hanada, H. Hamada and H. Nakauchi, 1996. Long-term lymphohematopoietic reconstitution by a single CD34-low/negative hematopoietic stem cell. Science, 273:242-245.
5. Bertoncello, I., G.S. Hodgson, T.R. Bradley, 1985. Multiparameter analysis of transplantable hemopoietic stem cells, I: the separation and enrichment of stem cells homing to marrow and spleen on the basis of Rhodamine-123 fluorescence. Exp. Hematol., 13: 999-1006.
6. Wolf, N.S., A. Kone, G.V. Priestley and S.H. Bartelmez, 1993. *In vivo* and *in vitro* characterization of long-term repopulating primitive hematopoietic cells isolated by sequential Hoechst, 33342-rhodamine123 FACS selection. Exp. Hematol., 21: 614-622.
7. Goodell, M.A., K. Brose, G. Paradis, A.S. Conner and R.C. Mulligan, 1996. Isolation and functional properties of murine hematopoietic stem cells that are replicating *in vivo*. J. Exp. Med., 183: 1797-1806.
8. Zhou, S., J.D. Schuetz, K.D. Bunting, A.M. Colapietro, J. Sampath, J.J. Morris, I. Lagutina, G.C. Grosveld, M. Osawa, H. Nakauchi and B.P. Sorrentino, 2001. The ABC transporter Bcrp1/ABCG2 is expressed in a wide variety of stem cells and is a molecular determinant of the side-population phenotype. Nat. Med., 7: 1028-1034.
9. Uchida, N., F.Y.K. Leung and C.J. Eaves, 2002. Liver and marrow of adult mdr-1a/1b-/- mice show normal generation, function and multi-tissue trafficking of primitive hematopoietic cells. Exp. Hematol., 30: 862-869.
10. Zhou, S., J.J. Morris, Y. Barnes, L. Lan, J.D. Schuetz, B.P. Sorrentino, 2002. Bcrp1 gene expression is required for normal numbers of side population stem cells in mice andconfers relative protection to mitoxantrone in hematopoietic cells *in vivo*. Proc. Natl. Acad. Sci. USA., 99: 12339-12344.
11. Matsuzaki, Y., K. Kinjo, R.C. Mulligan and H. Okano, 2004. Unexpectedly efficient homing capacity of purified murine hematopoietic stem cells. Immunity, 20: 87-93.
12. Nakauchi, H., K. Sudo and H. Ema, 2001. Quantitative assessment of the stem cell self-renewal capacity. Ann. N.Y. Acad. Sci., 938: 18-24.
13. Petzer, A.L., P.W. Zandstra, J.M. Piret and C.J. Eaves, 1996. Differential cytokine effects on primitive (CD34+CD38-) human hematopoietic cells: novel responses to Flt3-ligand and thrombopoietin. J. Exp. Med., 183: 2551-2558.
14. Sitnicka, E., N. Lin, G.V. Priestley, N. Fox, V.C. Broudy, N.S. Wolf and K. Kaushansky, 1996. The effect of thrombopoietin on the proliferation and differentiation of murine hematopoietic stem cells. Blood, 87: 4998-5005.
15. Kitamura, Y., T. Kasugai, N. Arizono, H. Matsuda, 1993. Development of mast cells and basophils: processes and regulation mechanisms. Am. J. Med. Sci., 306: 185-191.
16. Alexander, W.S., A.W. Roberts, N.A. Nicola, R. Li and D. Metcalf, 1996. Deficiencies in progenitor cells of multiple hematopoietic lineages and defective megakaryocytopoiesis in mice lacking the thrombopoietic receptor c-Mpl. Blood, 87: 2162-2170.

17. Kimura, S., A.W. Roberts, D. Metcalf and W.S. Alexander, 1998. Hematopoietic stem cell deficiencies in mice lacking c-Mpl, the receptor for thrombopoietin. Proc. Natl. Acad. Sci. USA., 95: 1195-1200.
18. Ueda, T., K. Tsuji, H. Yoshino, Y. Ebihara, H. Yagasaki, H. Hisakawa, T. Mitsui A. Manabe R. Tanaka, K. Kobayashi, M. Ito, K. Yasukawa and T. Nakahata, 2000. Expansion of human NOD/SCID-repopulating cells by stem cell factor, Flk2/Flt3 ligand, thrombopoietin, IL-6 andsoluble IL-6 receptor. J. Clin. Invest., 105: 1013-1021.
19. Eaves, C.J., J.D. Cashman and R.J. Kay, 1991. Mechanisms that regulate the cell cycle status of very primitive hematopoietic cells in long-term human marrow cultures. II. Analysis of positive and negative regulators produced by stromal cells within the adherent layer. Blood, 78: 110-117.
20. Nemunaitis, J., C.K. Tompkins, D.F. Andrews and J.W. Singer, 1991. Transforming growth factor beta expression in human marrow stromal cells. Eur. J. Hematol., 46: 140-145.
21. Moore, S.C., S.A. Theus and J.B. Barnett, 1992. Bone marrow natural suppressor cells inhibit the growth of myeloid progenitor cells and the synthesis of colony-stimulating factors. Exp. Hematol., 20: 1178-1183.
22. Hatzfeld, J., M.L. Li, E.L. Brown, H. Sookdeo., J.P. Levesque, T. O' Toole, C. Gurney, S.C. Clark and A. Hatzfeld, 1991. Release of early human hematopoietic progenitors from quiescence by antisense transforming growth factor beta 1 or Rb oligonucleotides. J. Exp. Med., 174: 925-929.
23. Fan, X., G. Valdimarsdottir, J. Larsson, A. Brun, M. Magnusson and S.E. Jacobse *et al.*, 2002. Transient disruption of autocrine TGF-beta signaling leads to enhanced survival and proliferation potential in single primitive human hemopoietic progenitor cells. J. Immunol., 168: 755-762.
24. Cardoso, A.A., M.L. Li, P. Batard, A. Hatzfeld, E.L. Brown, J.P. Levesque, H. Sookdeo, B. Panterne, P. Sansilvestri, S.C. Clark and J. Hatzfeld, 1993. Release from quiescence of CD34+ CD38- human umbilical cord blood cells reveals their potentiality to engraft adults. Proc. Natl. Acad. Sci. USA., 90: 8707-8711.
25. Li, M.L, A.A. Cardoso, P. Sansilvestri, A. Hatzfeld, E.L. Brown, H. Sookdeo, J.P. Levesque, S.C. Clark, and J. Hatzfeld, 1994. Additive effects of steel factor and antisense TGF-beta 1 oligodeoxynucleotide on CD34+ hematopoietic progenitor cells. Leukemia, 8: 441-445
26. Fortunel, N., J. Hatzfeld, S. Kisselev, M.N. Monier, K. Ducos, A. Cardoso, P. Batard and A. Hatzfeld, 2000. Release from quiescence of primitive human hematopoietic stem/progenitor cells by blocking their cell-surface TGF-beta type II receptor in a short-term *in vitro* assay. Stem Cells, 18: 102-111.
27. Datto, M.B., Y. Li, J.F. Panus, D.J. Howe, Y. Xiong and X.F. Wang, 1995 Transforming growth factor beta induces the cyclin-dependent kinase inhibitor p21 through a p53-independent mechanism. Proc. Natl. Acad. Sci. USA, 92: 5545-5549.
28. Landesman, Y., F. Bringold, D.D. Milne and D.W. Meek, 1997. Modifications of p53 protein and accumulation of p21 and gadd45 mRNA in TGF-beta 1 growth inhibited cells. Cell Signal, 9: 291-298.
29. Miyazaki, M., R. Ohashi, T. Tsuji, K. Mihara, E. Gohda and M. Namba, 1998. Transforming growth factor-beta 1 stimulates or inhibits cell growth via down- or up-regulation of p21/Waf1. Biochem. Biophys. Res. Commun., 246: 873-880.
30. Li, C.Y., L. Suardet and J.B. Little, 1995. Potential role of WAF1/Cip1/p21 as a mediator of TGF-beta cytoinhibitory effect. J. Biol. Chem., 270: 4971-4974.
31. Elbendary, A., A. Berchuck, P. Davis, L. Havrilesky, R.C. Bast and J.D. Jr., Iglehart *et al.*, 1994. Transforming growth factor beta 1 can induce CIP1/WAF1 expression independent of the p53 pathway in ovarian cancer cells. Cell Growth Differ., 5: 1301-1307.
32. Ducos, K., B. Pantern, N. Fortunel, A. Hatzfeld, M.N. Monier and J. Hatzfeld, 2000. p21(cip1) mRNA is controlled by endogenous transforming growth factor-beta1 in quiescent human hematopoietic stem/progenitor cells. J. Cell Physiol., 184: 80-85.
33. Fortunel, N.O., A. Hatzfeld and J.A. Hatzfeld, 2000. Transforming growth factor-beta: pleiotropic role in the regulation of hematopoiesis. Blood., 96: 2022-2036.
34. Cheng, T., H. Shen, N. Rodrigues, S. Stier and D.T. Scadden, 2001. Transforming growth factor beta 1 mediates cell-cycle arrest of primitive hematopoietic cells independent of p21(Cip1/Waf1) or p27(Kip1). Blood, 98: 3643-3649.
35. Hannon, G.J. and D. Beach, 1994. p15INK4B is a potential effector of TGF--induced cell cycle arres. Nature, 371: 257-261.
36. Li, J.M., M.A. Nichols, S. Chandrasekharan, Y. Xiong and X.F. Wang, 1995. Transforming growth factor beta activates the promoter of cyclin-dependent kinase inhibitor p15INK4B through an Sp1 consensus site. J. Biol. Chem., 270: 26750-26753.